

# The Application of a Seismo - and Chronostratigraphic Approach to Investigating Evidence of Paleoseismicity in Eastern Canada

NWMO-TR-2017-03

December 2017

**Gregory R. Brooks**

Natural Resources Canada, Geological Survey of Canada

**nwmo**

NUCLEAR WASTE  
MANAGEMENT  
ORGANIZATION

SOCIÉTÉ DE GESTION  
DES DÉCHETS  
NUCLÉAIRES



**Nuclear Waste Management Organization**

22 St. Clair Avenue East, 6<sup>th</sup> Floor

Toronto, Ontario

M4T 2S3

Canada

Tel: 416-934-9814

Web: [www.nwmo.ca](http://www.nwmo.ca)

# **The Application of a Seismo - and Chronostratigraphic Approach to Investigating Evidence of Paleoseismicity in Eastern Canada**

**NWMO-TR-2017-03**

December 2017

**Gregory R. Brooks**

Natural Resources Canada, Geological Survey of Canada

This report has been prepared under contract to NWMO. The report has been reviewed by NWMO, but the views and conclusions are those of the authors and do not necessarily represent those of the NWMO.

All copyright and intellectual property rights belong to NWMO.

### Document History

Title:	The Application of a Seismo - and Chronostratigraphic Approach to Investigating Evidence of Paleoseismicity in Eastern Canada		
Report Number:	TR-2017-03		
Revision:	R000	Date:	December 2017
Author Company(s)			
Authored by:	Gregory R. Brooks (Natural Resources Canada, Geological Survey of Canada)		
Verified by:	Hazen Russell		
Approved by:	Michael Lewis		
Nuclear Waste Management Organization			
Reviewed by:	Richard Crowe		
Accepted by:	Mark Jensen		

**ABSTRACT**

**Title:** The Application of a Seismo - and Chronostratigraphic Approach to Investigating Evidence of Paleoseismicity in Eastern Canada  
**Report No.:** NWMO-TR-2017-03  
**Author(s):** Gregory R. Brooks  
**Company:** Natural Resources Canada, Geological Survey of Canada  
**Date:** December 2017

**Abstract**

An integrated seismo - and chronostratigraphic investigation at Lac Dasserat, northwestern Quebec, identified 74 separate failures within eight event horizons. Horizons E and B, and H and G have strong or moderately-strong multi-landslide signatures, respectively, composed of 11 to 23 failures, while horizons F, D, C, and A have minor landslide signatures consisting of a single or pair of deposit(s). Cores collected at six sites recovered glacial Lake Ojibway varve deposits that are interbedded with the event horizons. The correlation of the varves to the regional Timiskaming varve series allowed varve ages or ranges of varve ages to be determined for the event horizons. Horizons H, G, E, and B are interpreted to be evidence of paleoearthquakes with differing levels of interpretative confidence, based on the relative strength of the multi-landslide signatures, the correlation to other disturbed deposits of similar age in the region, and the lack or possibility of alternative aseismic mechanisms. The four interpreted paleoearthquakes occurred between  $9770 \pm 200$  and  $8470 \pm 200$  cal yr BP, when glacial Lake Ojibway was impounded behind the Laurentide Ice Sheet during deglaciation. If correct, the interpreted paleoearthquakes identified in this study represent a Canadian example of elevated seismicity, associated with relatively rapid crustal unloading during deglaciation that occurred within an area of low historical seismicity.



## TABLE OF CONTENTS

	Page
ABSTRACT .....	iii
1. INTRODUCTION.....	1
2. STUDY AREA.....	2
3. METHODOLOGY.....	4
3.1    SUB-BOTTOM ACOUSTIC FACIES .....	6
3.2    LACUSTRINE FACIES .....	6
3.3    GLACIOLACUSTRINE FACIES .....	7
3.4    LANDSLIDE FACIES.....	7
4. EVENT HORIZONS .....	11
5. CORE DEPOSITS.....	12
6. VARVE THICKNESS RECORD .....	15
6.1    EVENT HORIZON VARVE AGES .....	16
7. DISCUSSION.....	19
8. CONCLUSIONS.....	27

## LIST OF TABLES

	Page
Table 1: Summary of Lac Dasserat coring sites and targeted deposits (see Fig. 2 for locations).....	6
Table 2: Cross-correlation statistics of the Dasserat varve record (1039-1637) compared to selected records of the Timiskaming varve series (see Fig. 7 for plots of the records).....	16
Table 3: Interpreted varve ages and inferred radiocarbon ages for the Lac Dasserat event horizons.....	17
Table 4: Assessment of possible aseismic mechanisms in glacial Lake Ojibway for event horizons H, G, and E.....	20
Table 5: Listing of youngest varve overlying disturbed glaciolacustrine deposits at sites in region, as reported in literature. See Fig. 9 for map of locations.....	21
Table 6: Qualitative levels of interpretative confidence that event horizons E, G, H, and B within Lac Dasserat were triggered by paleoearthquakes.....	26

## LIST OF FIGURES

	Page
Figure 1: Map showing the study area location within eastern Canada and with respect to the historical seismicity of the Western Quebec Seismic Zone. B) Map showing the Lac Dasserat study area, northwestern Quebec.....	3
Figure 2: Map of the Lac Dasserat survey area showing the sub-bottom acoustic profiling lines collected with the 15 (black lines) and 3.5 (red lines) kHz low frequency transducers. Also shown are the locations of the six coring sites (see Table 1) and the three profiles depicted in Fig. 3.....	5
Figure 3: Three examples of interpreted (A, B, and C) and uninterpreted (A', B', and C') sub-bottom acoustic profiles collected with the 15 kHz LF transducer showing the lacustrine, glaciolacustrine, and landslide facies; refer to Fig. 2 for profile locations. 8	8
Figure 4: Shaded-relief maps depicting the lateral extent and thickness of the submarine landslide deposits for the eight event horizons. The arrows on the maps represent the interpreted direction of mass movement flow.....	10
Figure 5: Logs of the six recovered cores; see Fig. 2 for coring locations. The recovered cores penetrated all four of the multi-landslide event horizons (H, G, E, and B) as well as horizon F.....	13
Figure 6: Radiographs of selected portions of the Lac Dasserat cores showing examples of lacustrine, glaciolacustrine, and landslide deposits.....	14
Figure 7: Plots of the varve thickness versus numbering for the Dasserat varve record as well as for lakes Duparquet and Montbeillard, and the Timiskaming A7, B7-B8a, and F5-F6-F7-F8 records (data courtesy of A. Breckenridge.....	15
Figure 8: Plot of the varve ages (or age ranges) of the event horizons superimposed over a timescale that spans varve sedimentation in glacial Lake Ojibway and the post-glacial lake period.....	18
Figure 9: Map showing the locations of varve sampling sites of Antevs (1925, 1928), Hughes (1959), and Breckenridge et al. (2012). .....	25

## 1. INTRODUCTION

Numerous studies demonstrate that late Holocene lake bottom deposits can contain multiple submarine landslide and/or turbidity current deposits at a common stratigraphic level that formed during modern or historical earthquakes (Shilts, 1984; Shilts and Clague, 1992; Siegenthaler et al., 1987; Chapron et al., 1999; Nomade et al., 2005). Occurrences of such multi-deposit signatures within prehistoric portions of lake sediments have also been interpreted to be evidence of paleoearthquakes (Schnellmann et al., 2002; Strasser et al., 2013). Because of the high potential for deposit preservation, paleoseismic investigations of lake deposits have yielded long-term earthquake records at many locations globally (e.g., Doig, 1990, 1998; Karlin et al., 2004; Becker et al., 2005; Monecke et al., 2006; Schnellmann et al., 2006; Upton and Osterberg, 2007; Moernaut et al., 2007, 2014; Bertrand et al., 2008; Anselmetti et al., 2009; Beck, 2011; Morey et al., 2013; Smith et al., 2013; Strasser et al., 2013; Kremer et al., 2015; Praet et al., 2016). Studies of lake deposits are especially applicable to intracratonic areas where primary evidence of paleoseismicity can be difficult to recognize (Stewart et al., 2000).

During the recession of the Laurentide Ice Sheet, substantial areas of eastern Canada were inundated by large glacial lakes or by extensions of the sea onto isostatically depressed areas (Dyke et al., 2003). These water bodies subsequently drained or receded, but thick accumulations of glaciolacustrine and glaciomarine deposits are preserved in modern lakes basins (e.g., Kaszycki, 1987; Lazorek et al., 2006; Brooks and Mediolli, 2012; Normandeau et al., 2013; Eyles et al., 2015). Submarine landslide deposits have been recognized within glaciolacustrine or early post-glacial lacustrine deposits and some have been interpreted to be evidence of paleoearthquakes (Adams, 1982; Shilts et al., 1992; Ouellet, 1997; Doughty et al., 2014; Lajeunesse et al., 2016). The latter landslide deposits may be evidence of deglacial seismicity that is related to crustal unloading from the retreat of the ice sheet. Although elevated deglacial seismicity in areas of low historical seismicity is well established in Fennoscandia, as indicated by fault scarps, subaerial landslides, liquefaction structures, and tsunami layers (Lundqvist and Lagerbäck, 1976; Lagerbäck, 1990; Mörner, 2003, 2004, 2005; Smith et al., 2014), there are no similar well-documented examples in eastern Canada (Adams, 1989, 1996; Johnston, 1996; Stewart et al., 2000).

Investigating paleoseismicity is important to understanding the long term seismic hazard of the intracratonic setting of eastern Canada, which is poorly understood in part because the instrumental and historical records of earthquakes are short, spanning very locally only into the 17<sup>th</sup> century (Gouin, 2001; Lamontagne et al., 2008). Lake basins in eastern Canada containing interbedded submarine landslide deposits within well-stratified glaciolacustrine or glaciomarine deposits are ideal locations to apply an integrated seismo- and chrono-stratigraphic methodology that has been used successfully to investigate younger post-glacial paleoseismicity elsewhere (Brooks, 2015).

This report assesses the possible seismogenic origin of submarine landslide deposits within the late glacial stratigraphy of Lac Dassurat, northwestern Quebec (Fig. 1). The interpretations utilize sub-bottom acoustic profiling data collected within a high-density sampling grid to map eight landslide event horizons in the upper portion of the lake stratigraphy. Glaciolacustrine varve deposits that are interbedded with the mapped landslide beds provide chronological control. As presented below, four multi-deposit event horizons are interpreted as evidence of paleoearthquakes with differing levels of interpretative confidence; aseismic origins best explain the four single and paired deposit horizons. This study, thus, presents evidence of

paleoseismicity that occurred during deglaciation within an area previously inundated by a large glacial lake and which experienced a low level of historical seismicity.

## 2. STUDY AREA

Lac Dasserat, Quebec, is located ~425 km northwest of Ottawa, Ontario (Fig. 1A). The lake covers ~28 km<sup>2</sup>, is up to 12.4 km long, 6.5 km wide and 17 m deep. Typical of many lakes on the Canadian Shield, the lake is irregular in shape and the bathymetry reflects the relief of the underlying bedrock. The immediately surrounding area consists of hilly terrain with relief up to 20 m high. The local surficial geology is mapped predominately as deep water glaciolacustrine sediments with numerous outcrops of bedrock, pockets of glacial deposits, and wetlands (Veillette et al. 2010). Submarine landslide deposits within Lac Dasserat were discovered initially within sub-bottom acoustic profile returns collected for an investigation of environmental metal contamination from a nearby former mining site (Alpay, 2016).

Lac Dasserat is located within an intracratonic setting ~150 km north of the concentrated belt of historical seismicity within the Western Quebec Seismic Zone, which encompasses parts of western Quebec, eastern Ontario, and northern New York State (Fig.1A; Basham et al., 1982; Adams and Basham, 1989, 1991). The 1935 Temiskaming earthquake (*M* 6.1) is the most significant historical earthquake within the northern portion of the seismic zone (Lamontagne et al., 2008); its epicenter is located about 165 km to the south of Lac Dasserat.

The lake is situated within a large area of northwestern Quebec-northeastern Ontario that was inundated by a glacial lake impounded against the retreating Laurentide Ice Sheet located to the north. This water body, referred to at different stages as lakes Barlow, Barlow-Ojibway and Ojibway, evolved within the isostatically-depressed landscape of the Timiskaming and Hudson Bay basins between roughly 11.0 and 8.4 ka cal BP (Vincent and Hardy 1979; Veillette 1994; Dyke et al., 2003; Breckenridge et al., 2012; Roy et al. 2015)). The succession of lake stages ended when glacial Lake Ojibway, which existed in the area north of the modern drainage divide, drained catastrophically northwards into the James and Hudson basins through a breach in the impounding Laurentide Ice Sheet (Hardy, 1982; Barber et al., 1999; Roy et al. 2011; Daubois et al., 2015).

The Lac Dasserat area was inundated by proglacial lake water, up to ~80 m deep, during the Temiskaming and Anglier phases of glacial lake sequence (Vincent and Hardy, 1979; Veillette, 1994). Water levels subsequently declined to the early and late Kinojévis phases, as the ice front retreated farther northwards and the landscape rebounded (Roy et al., 2015). During these later stages, the Dasserat basin was located initially within one of several low interfluvial areas that funneled outflow southward from glacial Lake Ojibway and later within one of several outlet channels (Vincent and Hardy, 1979).

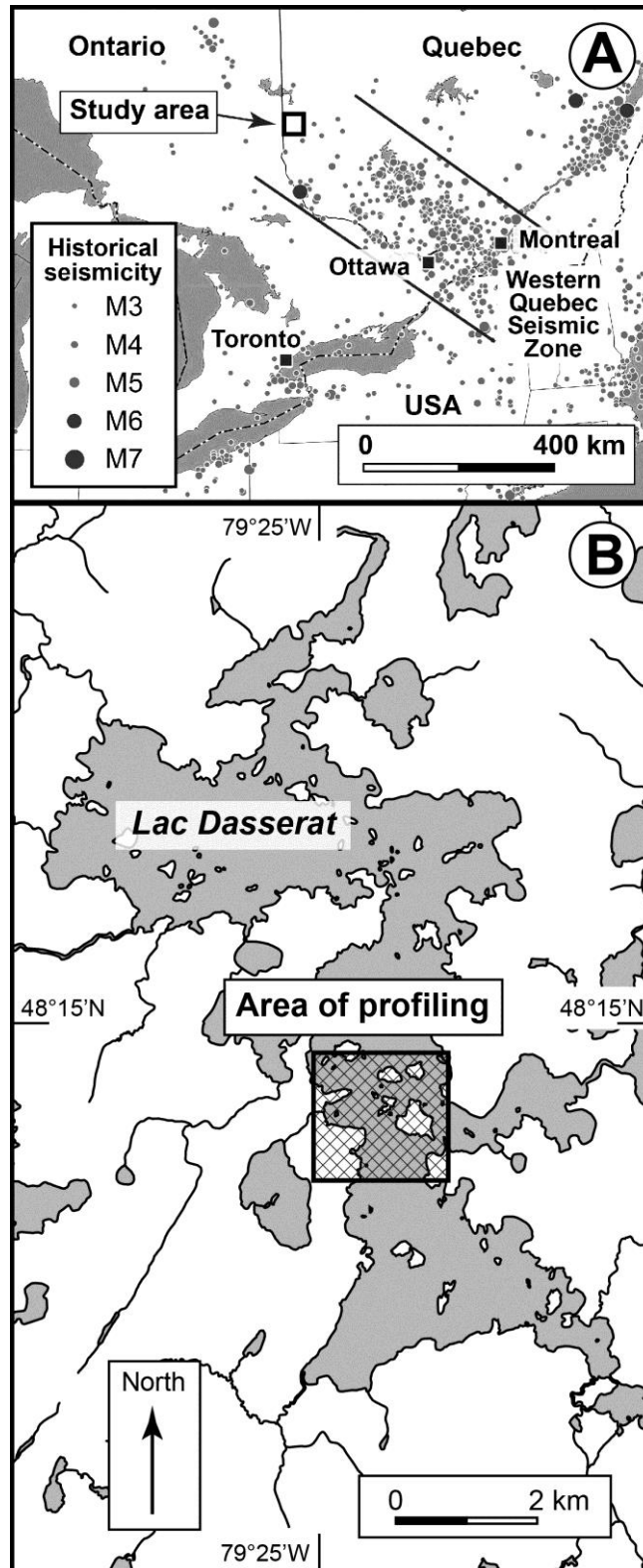


**Figure 1: Map showing the study area location within eastern Canada and with respect to the historical seismicity of the Western Quebec Seismic Zone. B) Map showing the Lac Dasserat study area, northwestern Quebec.**

A legacy of the glacial lakes is the regional occurrence of glaciolacustrine deposits that form the Great and Lesser clay belt areas of northwestern Quebec-northeastern Ontario. About 2100 rhythmic laminations within these deposits form the 'Timiskaming varve series' that was compiled by Antevs (1925, 1928), based on the correlation of varve thickness patterns from different locations throughout the region. Subsequent research verified the regional correlation of the varves, which are interpreted to be annual accumulations (Hughes, 1965; Breckenridge et al., 2012). Regional varve sedimentation is dated tentatively as occurring between  $10,570 \pm 200$  and  $8470 \pm 200$  cal yr BP (Breckenridge et al., 2012). The varves are time-transgressive, with the sequences being older in the south and younger in the north; no single location contains the entire varve series. Following the terminology of other studies in the area, the varves in Lac Dasserat are referred to as glacial Lake Ojibway deposits.

### 3. METHODOLOGY

Collected between September 9 and 17, 2014, the sub-bottom acoustic profiling survey of Lac Dasserat used a Knudsen CHIRP Pinger SBP™ echosounder system with low frequency (LF) 15 or 3.5 kHz and high frequency 200 kHz transducers mounted on the side of a 4.9 m (16 ft) aluminum boat powered by a 30 hp motor. Traversing speed during profiling ranged between 5 to 7 km.hr<sup>-1</sup>. A Trimble DSM232 GPS receiver-GA510 L1/L2/L band antenna collected differentially-corrected GPS data along the profiling routes, recorded in combination with the digital profiling data. The survey collected about 125 and 19 line-km of data using the 15 and 3.5 kHz LF transducers, respectively, over four sub-basins in the lower-middle area of Lac Dasserat that are informally referred as the south, middle, north and northeast basins (Figs. 1B and 2). Most of the profiles follow a grid pattern with the lines spaced 40 to 60 m apart, which permitted the detailed mapping of the stratigraphic position, thickness and extent of isolated or coalesced landslide deposits. The velocity of the acoustic energy in the water is assumed to be 1450 m.s<sup>-1</sup>.

Profile analysis used the 15 kHz data to map the upper eight, stratigraphic occurrences of the submarine landslide deposits that are sufficiently thick (i.e., greater than about 0.1 m) and laterally extensive enough to be identified unequivocally between several profiles. On each profile, horizon picking using KingdomSuite™ software delineated the top and bottom surfaces of each landslide deposit. The stratigraphic positions of the pinch-outs of the picked landslide deposits defined the levels of 'event horizons' within the lake stratigraphy. The x-y-z coordinates of points along the top and bottom surfaces of the landslide deposits within each event horizon were exported into and gridded using Surfer™, and then mapped and edited using GlobalMapper™ and Illustrator™. This yielded eight shaded-relief maps each depicting the extent and thickness of the landslide deposits within a given event horizon. Depending on the architecture of the sub-bottom, a given event horizon may be composed of one or more landslide deposit(s). Where multiple landslides are present, the constituent deposits are inferred to have happened synchronously within the resolution of the profiling returns.

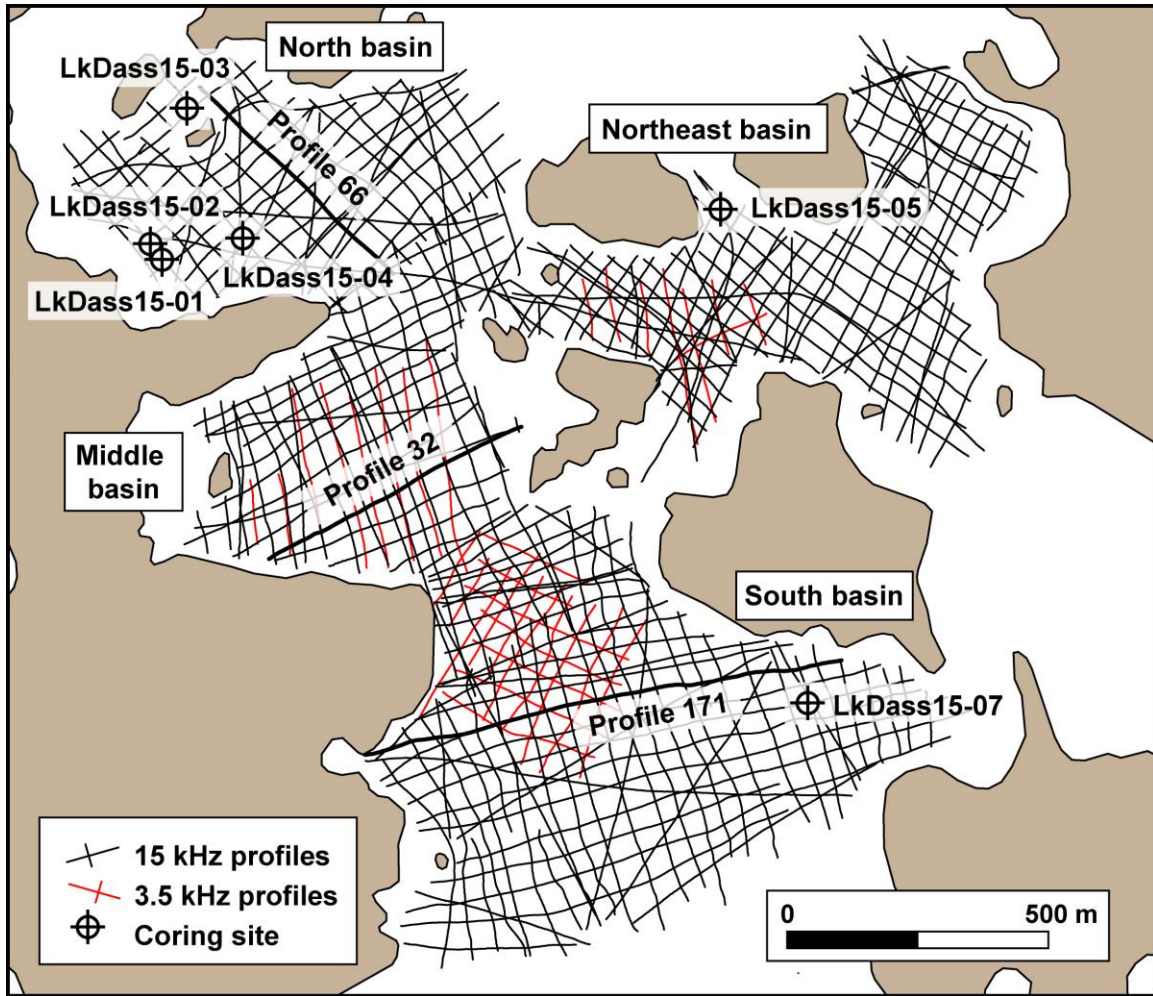


**Figure 2: Map of the Lac Dasserat survey area showing the sub-bottom acoustic profiling lines collected with the 15 (black lines) and 3.5 (red lines) kHz low frequency transducers. Also shown are the locations of the six coring sites (see Table 1) and the three profiles depicted in Fig. 3.**

Coring from an ice cover in March 2015 recovered interbedded glaciolacustrine and landslide deposits from six locations within the survey area (Fig. 2 and Table 1; Brooks, 2016a). Coring site selection targeted specific deposits of interest, whilst minimizing water depth and limiting coring depth to within 4 to 6 m of the lake bed. Locating the coring sites in the field used differentially-corrected GPS coordinates collected with a Novotel Smart-V1 antenna-receiver. Coring utilized a Livingston corer (Livingston, 1955) with 50.8 mm (O.D.) aluminum tubes that recovered sections of core 0.84 to 1.0 m long. Each sampling site consisted of a pair of recovered cores, located about one metre apart. The segments of the two cores have overlapping sampling depth intervals and thus contain a continuous, composite sample of the penetrated deposits. Immediately upon recovery, core tubes are sealed with plastic caps and taped securely, and then stored to prevent freezing.

**Table 1: Summary of Lac Dasserat coring sites and targeted deposits (see Fig. 2 for locations).**

Coring Site	Date of coring	Latitude	Longitude	Water depth (m)	Targeted deposits
LkDass15-01 (north basin)	March 17 and 19, 2015.	48.24171	-79.4153	2.83	Event horizons E and H
LkDass15-02 (north basin)	March 19, 2015	48.24197	-79.4156	3.05	Thick sequence of varves
LkDass15-03 (north basin)	March 13, 2015	48.2443	-79.4146	3.25	Event horizons E and F
LkDass15-04 (north basin)	March 15 and 18, 2015	48.24203	-79.4132	5.08	Event horizon B
LkDass15-05 (northeast basin)	March 14, 2015	48.24234	-79.4008	2.85	Event horizons E and G
LkDass15-07 (south basin)	March 20, 2015	48.23383	-79.3989	4.20	Event horizons E and G

CT-Scanning of the cores at the Institut national de la recherche scientifique, Quebec City, Quebec produced tomodesitometry radiographs of the recovered deposits. Visual identification of common distinctive varves in the radiographs allowed the correlation of varved deposits between overlapping core segments for each coring site (see Brooks, 2016a). Extending this process to the radiographs between different coring sites produced a continuous, composite varve series through the sequence of glaciolacustrine deposits.

Two people independently measured varve thicknesses along the composite series using full-scale, high-contrast, radiograph images, and the results then averaged (Zolitschka et al., 2015). The thicknesses are based on the visual interpretation of the top to bottom character of the varve couplets and the measurements made with the ruler tool in Illustrator™.

In the laboratory, split core were logged and subsampled for sediment texture, carbon content, and real sample XRF analyses (Girard et al. 2004).

### 3.1 SUB-BOTTOM ACOUSTIC FACIES

Three depositional acoustic facies are present within the profiling returns, as follows:

### 3.2 LACUSTRINE FACIES

This facies forms the youngest stratigraphic unit and is a drape, up to ~7 m thick, within the sub-basins. The facies thins and may pinch toward the shoreline or other shallowing areas (Fig. 3). Internally, the facies returns are transparent to weakly bedded; where present, bed spacing is of decimetre scale. Basal contact is defined by a strong impedance layer overlying

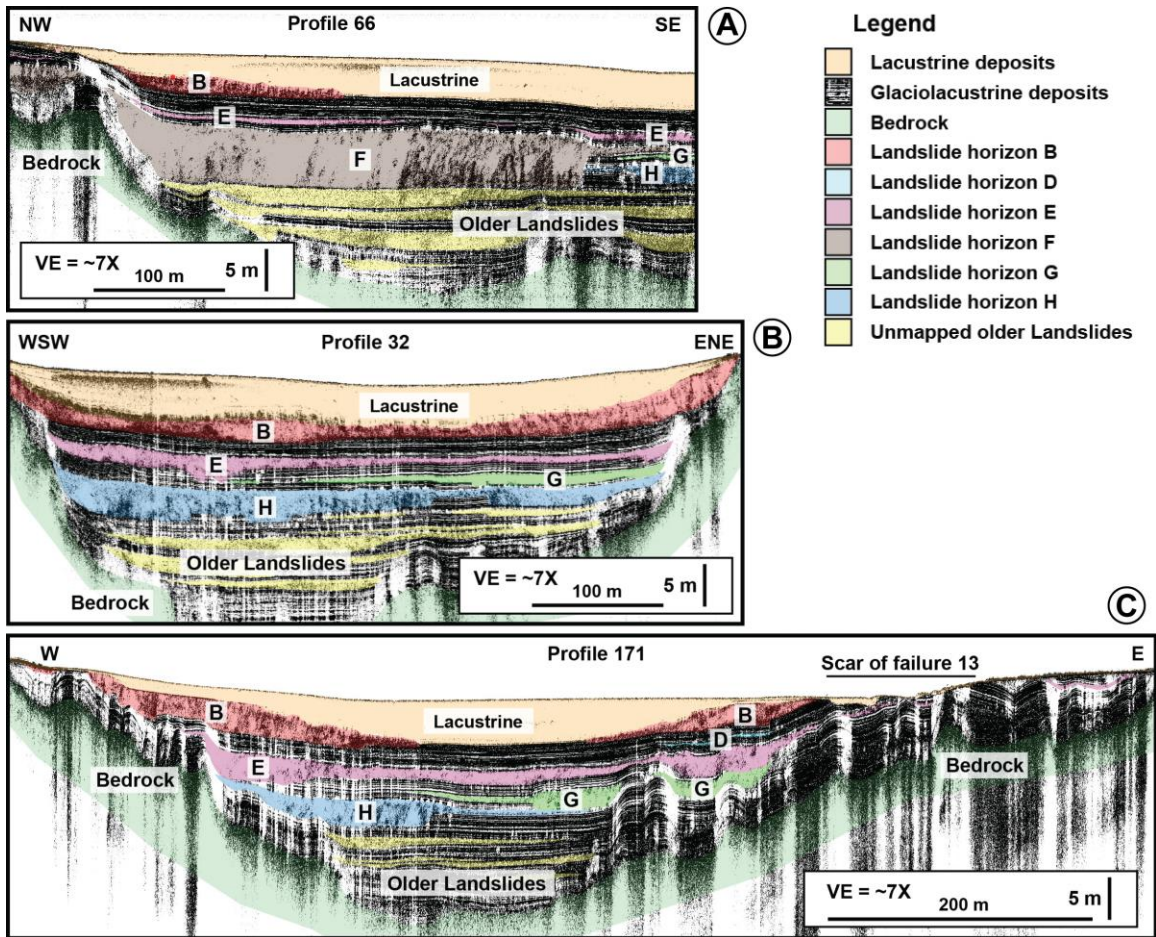
the glaciolacustrine facies, but is transitional locally, and indistinct or irregular where overlying the landslide facies. The basal surface is primarily conformable, but very locally is unconformable where the facies overlies apparent landslide scars. Deposits with similar acoustic facies are ubiquitous to lakes on the Canadian Shield and have been observed in many sub-bottom profiling surveys reported elsewhere, (e.g., Klassen and Shilts, 1982; Shilts, 1984; Kaszycki, 1987; Shilts et al., 1992; Brooks and Medioli, 2012; Lazorek et al., 2006; Normandeau et al., 2013; Doughty et al., 2010, 2013, 2014). This facies represents post-glacial lacustrine deposits in Lac Dasserat.

### **3.3 GLACIOLACUSTRINE FACIES**

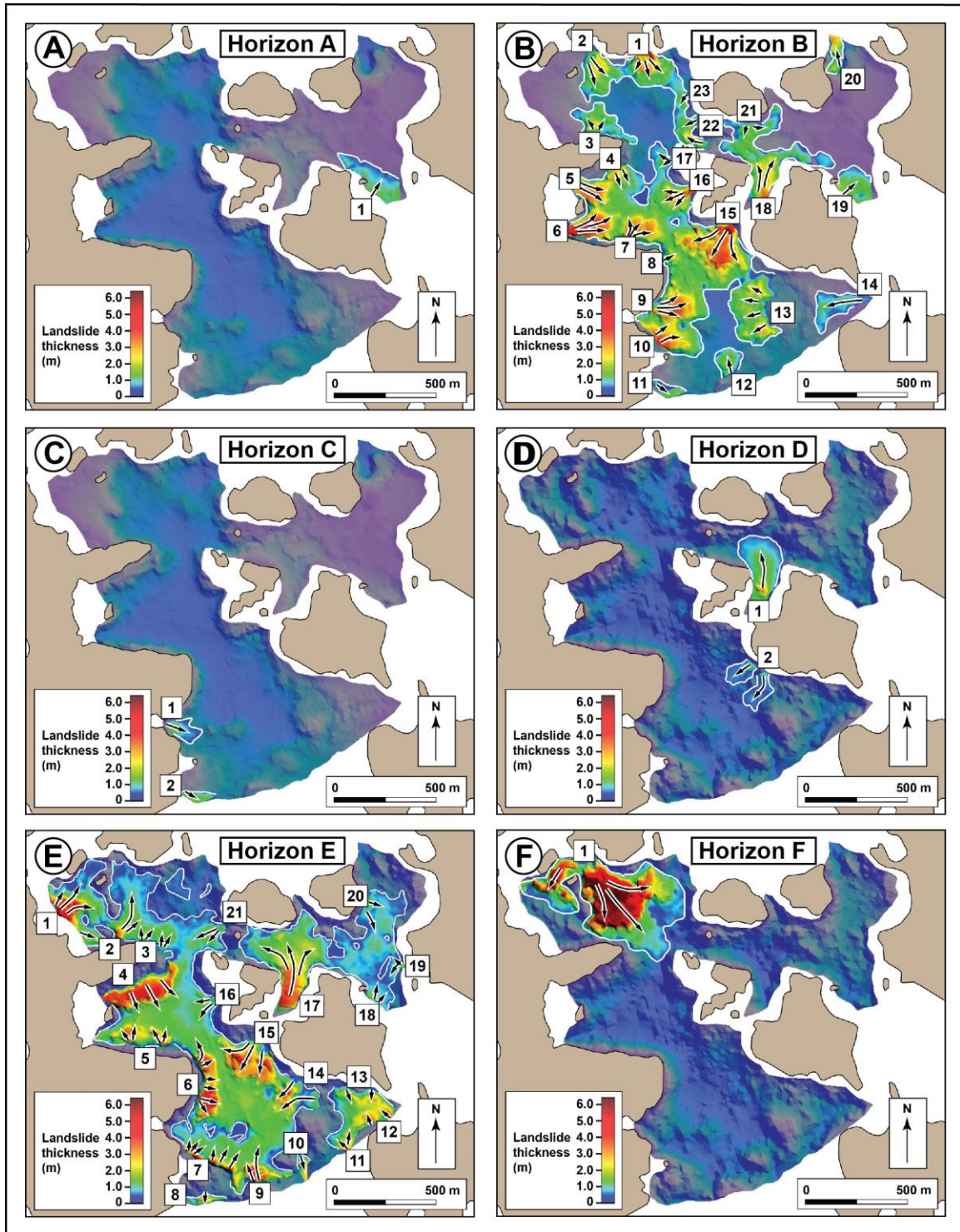
The returns of the glaciolacustrine facies exhibit well-defined, decimeter-scale, laterally continuous, parallel reflectors that are draped on the underlying topography (Fig. 3). The facies form multiple beds, up to several metres thick, that are interbedded with the landslide facies. The deposits thin and pinch out against the steeper sub-basin margins. Basal contact of the beds is mostly well-defined and conformable, but locally unconformities are present where beds on-lap onto steeper slopes from where older deposits have failed. Deposits exhibiting this acoustic facies are common to many lakes on the Canadian Shield and are the product of glaciolacustrine sedimentation (references cited above). The deposits forming the glaciolacustrine facies accumulated within glacial Lake Ojibway, as confirmed by the correlation of the constitute rhythmic laminations to the regional Timiskaming varve series (see below).

### **3.4 LANDSLIDE FACIES**

This facies forms multiple, gently undulating beds, up to 7 m thick, that constitute a significant portion of the sub-bottom within the sub-basins (Fig. 3). In profiles that extend perpendicular to the sub-basin sides, the beds are either wedge-shaped, being thicker against one shoreline and pinching-out across a sub-basin (Fig. 3C, landslide deposits B, G and H), or are thicker along opposite shorelines and thinning towards the middle area (Fig. 3B, deposits B, E and H). The facies beds are interbedded within the glaciolacustrine facies, except for the three stratigraphically-youngest beds, which are at the interface between the lacustrine and glaciolacustrine facies (landslide deposit B in Fig. 3 and deposits A, B and C in Fig. 4J).



**Figure 3: Three examples of interpreted (A, B, and C) and uninterpreted (A', B', and C') sub-bottom acoustic profiles collected with the 15 kHz LF transducer showing the lacustrine, glaciolacustrine, and landslide facies; refer to Fig. 2 for profile locations. Although event horizons H, G, E, and B are present in the three profiles, no single profile within the study area contains all eight of the mapped event horizons. Note, landslide deposits form a significant portion of the sub-bottom and that there are older unmapped deposits (shaded yellow) in the lower portion of the sub-bottom. In C), part of the profile crosses the source area scar of failure 13 of horizon B, as mentioned in the text.**



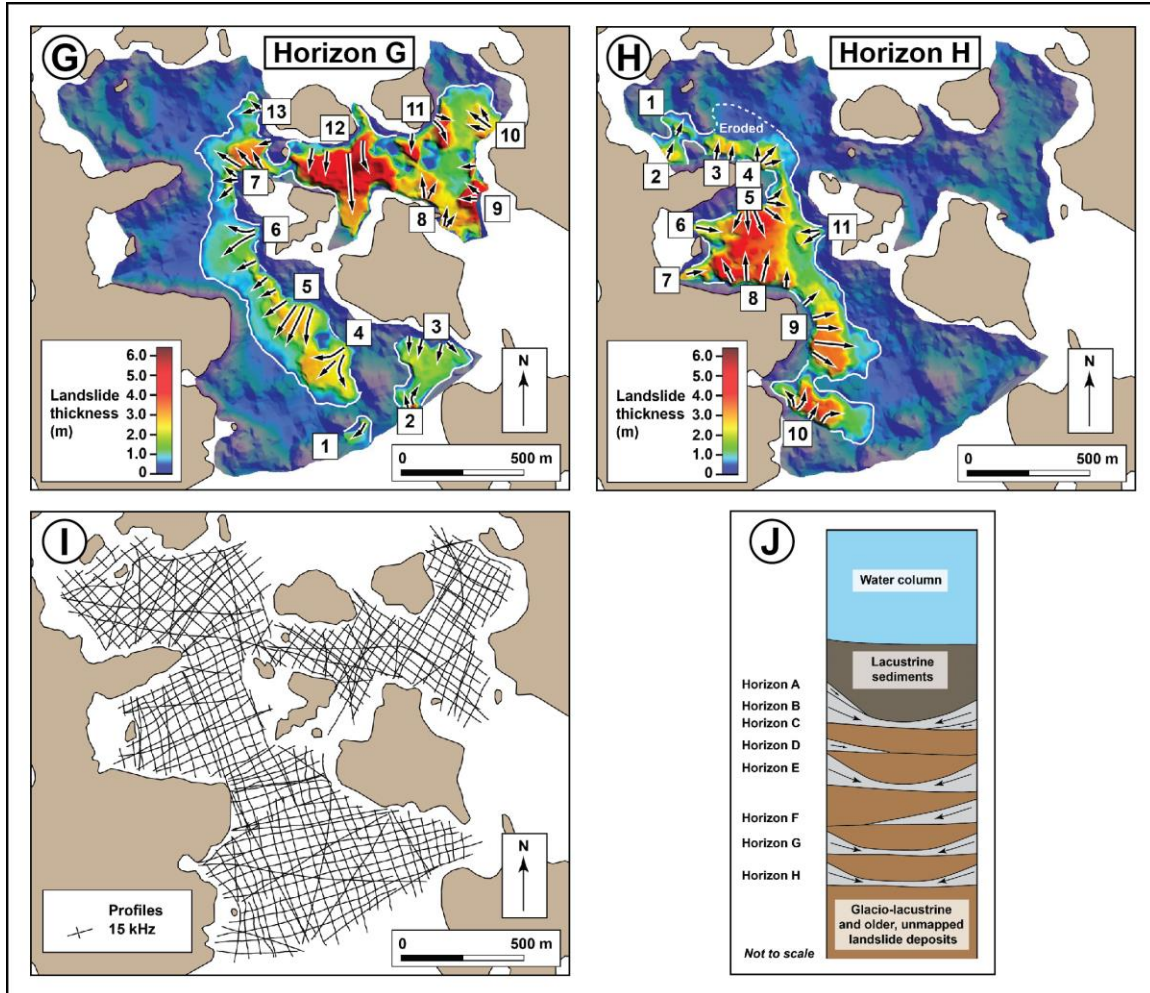


**Figure 4: Shaded-relief maps depicting the lateral extent and thickness of the submarine landslide deposits for the eight event horizons. The arrows on the maps represent the interpreted direction of mass movement flow. Landslide deposits interpreted to originate from separate source areas are numbered on each map. For reference, the map in I) shows the density of the 15 kHz profile lines from which the event horizon maps were compiled, and J) provides the relative stratigraphic context for the horizons. In H), the dashed line in the north basin represents the estimated extents of deposits 3 and 4 in horizon H that are truncated by the thick, overlying deposit of horizon F. Of note, the thicker areas of the deposits on the maps appear to be topographically high, but in fact these areas commonly have negative relief and are present where landslide debris eroded into the underlying deposits (e.g., landslide E in Fig. 3B and C).**

Internally, the facies beds lack continuous internal reflectors and appear transparent, diffuse or chaotic. Clasts of glaciolacustrine deposits with disoriented internal reflectors are present within the returns of some beds. The upper surface of the facies may be smooth to irregular; water escape(?) structures, up to 1 m high, several metres across and extending into overlying glaciolacustrine deposits, are present very locally in some profiles (e.g., along the top of deposit F in Fig. 3A). Along the sub-basin margins, where the individual facies beds are thickest, the basal contact commonly is erosive and truncates underlying glaciolacustrine and, in places,

older mass transport deposits (Fig. 3A - deposit F; 3B - deposits E and H; 3C - deposits E, G and H). Laterally, an erosive contact transitions to a conformable one as a bed thins.

Similar landslide facies have been documented by many lake studies elsewhere (e.g., Siegenthaler et al., 1987; Chapron et al. 1999; Monecke et al. 2006; Schnellmann et al., 2006; Bertrand et al., 2008; Moernat et al., 2007, 2014; Anselmetti et al., 2009; Strasser et al., 2013), including some on the Canadian Shield (e.g., Shilts and Clague, 1992; Shilts et al., 1992; Doughty et al., 2014). All of the submarine landslide deposits in the study area accumulated within glacial Lake Ojibway, except the stratigraphically youngest deposits, which occurred during the transition from a glacial to post-glacial lake.

#### 4. EVENT HORIZONS

Eight shaded-relief maps depicting the lateral extent and thickness of the landslide deposits within the event horizons, are shown in Fig. 4. Designated H to A from stratigraphically oldest to youngest, horizons H, G, F, E, and D are interbedded within glaciolacustrine deposits, while horizons C, B, and A are situated at the interface between the lacustrine and glaciolacustrine facies (Figs. 3 and 4J). The mapped event horizons are not a complete record of landslide deposits within Lac Dasserat, as there are older, unmapped deposits in the lower portion of the sub-bottom (yellow-shaded areas in Fig. 3).

The maps reveal that the majority of the 74 mapped landslide deposits fall within horizons H, G, E, and B, while the other four horizons (F, D, C, and A) contain one or two isolated deposits (Fig. 4). Event horizons E and B contain the most landslides with 21 and 23 deposits, respectively, and both represent strong, multi-landslide signatures relative to the other horizons. The deposits in both are widely distributed throughout the four sub-basins; many are coalesced and the lateral boundaries indistinguishable in the profile returns (Fig. 3).

Eleven and thirteen landslides are in event horizons H and G, respectively. The landslide deposits in horizon H are located predominately on the western side of the north, middle and south sub-basins, while those of horizon G are located in the northeast sub-basin and on the eastern portions of the north, middle and south sub-basins (Fig. 4G and H). In the north basin, a significant portion of the deposits labeled 3 and 4 within horizon H are truncated erosively by the thick landslide deposits of horizon F (Figs. 3A and 4H). Event horizons H and G both represent moderately-strong, multi-landslide signatures relative to the strong signatures of horizons E and B.

The single and paired landslide deposits of horizons C and A, respectively, directly under- and overlie the deposits of horizon B (Fig. 4A, C and J). It is unclear from the profiling returns if there are thin lacustrine or glaciolacustrine deposits separating the deposits that would indicate whether horizons C and A are distinctly separate temporally from B. Thus it is possible that the deposits of horizons C and A represent early and late phases of the same failure episode as those of horizon B. Whether they are or not is not deemed important to horizon B, as its 23 mapped failures clearly exhibit a strong multi-landslide signature.

The two landslides within horizon D are located within the northeast and south basins (Fig. 4D). The thickest and most laterally extensive landslide within the study area is the single deposit ( $\sim 8 \times 10^5 \text{ m}^3$ ) that forms horizon F and originates from the north-side of the north basin. Overall, the single and paired landslide deposits of horizons D, C, and A represent minor signatures in the study area stratigraphy relative to those of horizons H, G, E, and B. Horizon F

is also considered to be a minor horizon because it is composed of a single deposits present only in the north basin, albeit one that is product of a substantial failure.

## 5. CORE DEPOSITS

Cores LkDass15-01, -03, -04, -05 and -07 targeted the deposits of event horizons B, E, F, G, and/or H (Table 1; Fig. 2). Core LkDass15-02 collected a thick sequence of glaciolacustrine sediments to aid correlating the Lac Dasserat varves to the regional Timiskaming varve series. This core did not reach the bottom of the glaciolacustrine deposits, but it did penetrate a thin bed of horizon H, which is the lateral extension of the same deposit in core LkDass15-01 (Figs. 2, and 5).

The recovered cores contain lacustrine, glaciolacustrine and landslide deposits, consistent with the profiling returns (Fig. 5). All are composed of clay-silt, except for a very fine sand bed, 0.08 m thick, in core LkDass15-04 between the top of the glaciolacustrine sediments and the overlying landslide deposit of horizon B (Figs. 5 and 6B). No organic materials relevant to the aggradation of the deposits were found in the cores.

In the radiographs, the varved glaciolacustrine deposits are composed of denser, silt-rich, summer layers that are lighter shaded than the thicker, darker-toned, clay-rich, winter layers (Fig. 6). Internal contact between the summer and winter layers is gradational; contact between successive couplets is sharp to gradational and can be planar to irregular in geometry at the millimeter scale. The glaciolacustrine deposits lack dropstones, or even sand-sized grit, that might represent ice-rafted debris, except for several pea-sized dropstones. It is inferred that the rarity of ice-rafted debris and the clay-silt texture of the couplets indicates that the varves represent distal sedimentation within glacial Lake Ojibway with respect to sediment sources located presumably along the margin of the impounding Laurentide Ice Sheet to the north.

Varve thicknesses range from 5 to 31.6 mm over most of recovered cores (Fig. 7). The thicknesses become less than 4 mm in the uppermost 0.1 m of the varve sequence in core LkDass16-04, where individual couplets become increasingly disturbed vertically by core sampling and difficult to differentiate unequivocally (Figs. 5 and 6B). This disturbance was caused by hammering the core tube through the sand bed that directly overlies the top of the varve deposits (Figs. 5 and 6B).

The landslide deposits in the recovered cores range from 0.025 to ~1.5 m thick, although coring did not completely penetrated the deepest beds in cores LkDass15-01, -03, -05 and -07 (Fig. 5). The deposits are composed of resedimented glaciolacustrine deposits that include blocks of tilted or deformed rhythmites, brecciated varve debris, and sheared and faulted varves (Fig. 6). The contacts between the lacustrine or glaciolacustrine deposits and the underlying landslide beds are sharp and well defined on the core radiographs.

Although widespread throughout the study area in the profiling returns, only two cores contained lacustrine deposits (LkDass15-04 and to lesser extent LkDass15-05), reflecting coring site selection that targeted the interbedded glaciolacustrine and landslide deposits. In the radiographs, the lacustrine deposits exhibit mottling from bioturbation (Fig. 6A). In split core, the olive-grey lacustrine deposits appear massive.

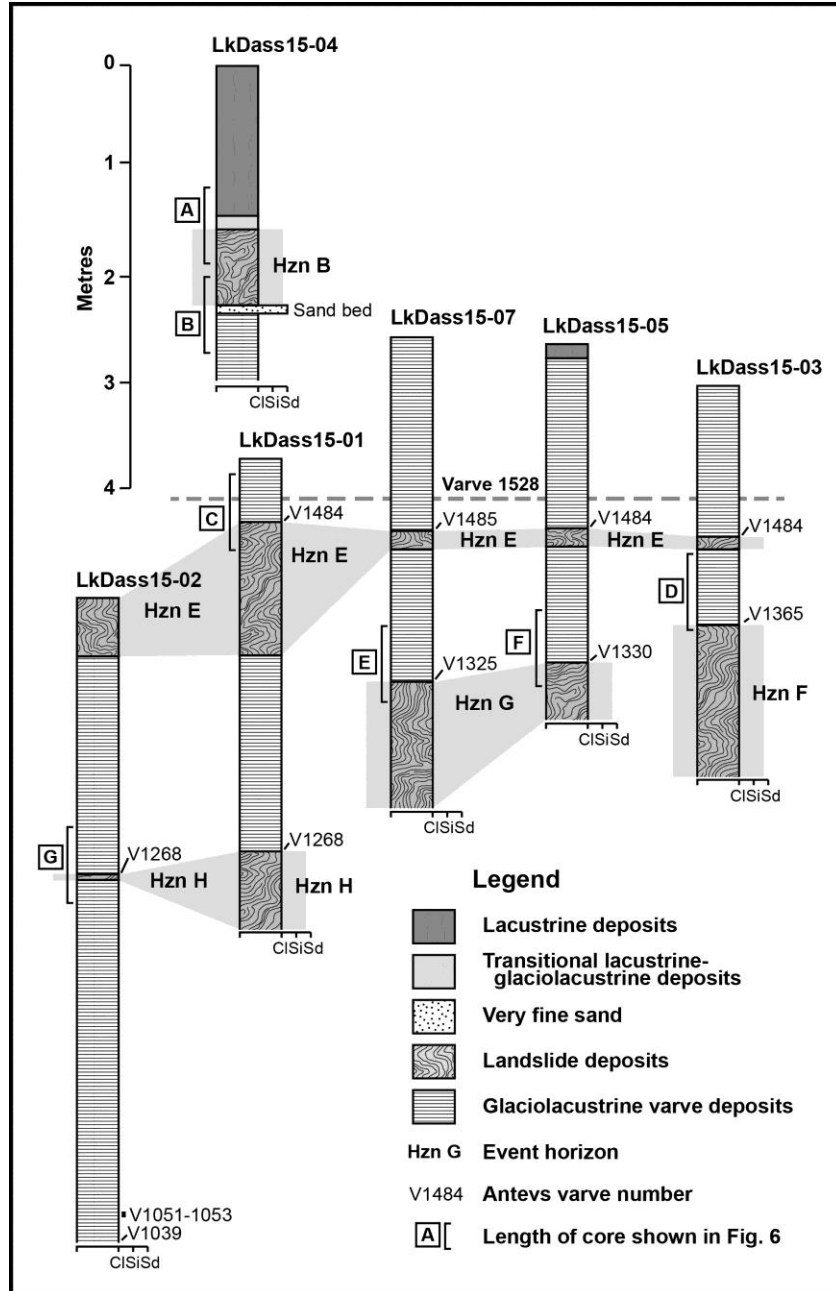


**Figure 5: Logs of the six recovered cores; see Fig. 2 for coring locations. The recovered cores penetrated all four of the multi-landslide event horizons (H, G, E, and B) as well as horizon F. The Timiskaming varve series number is shown for the first varve overlying horizons H, G, F, and E. Also shown is the position of varve 1528, which is a regionally distinctive varve within the Timiskaming varve series. The lack of landslide deposits below horizon H in core LkDass 15-02 reflects the selected coring site, which targeted a long varve sequence, and does not imply an absence of landslide deposits below horizon H in the study area. There is strong microfracturing in core LkDass15-02 between varves 1051-1053, as mentioned in the text.**

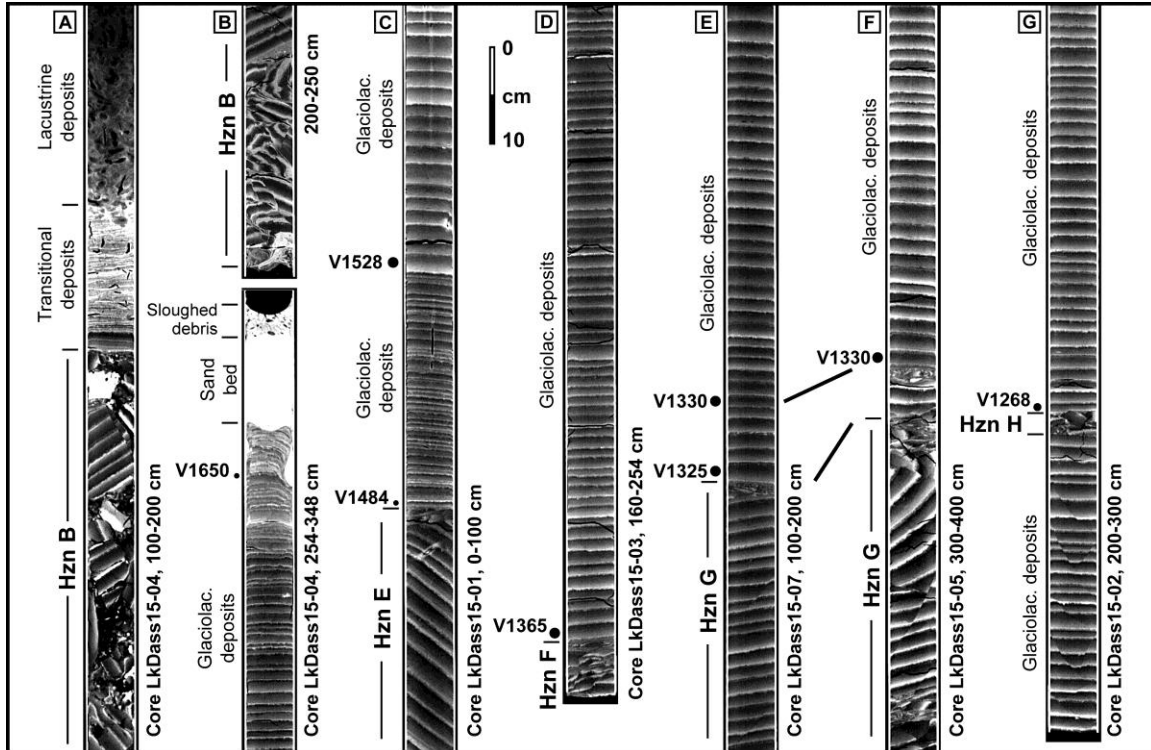


**Figure 6: Radiographs of selected portions of the Lac Dasserat cores showing examples of lacustrine, glaciolacustrine, and landslide deposits; see Fig. 2 for coring site locations and Fig. 5 for the location of the radiographs on the composite logs. Note, the landslide deposits (labeled by event horizons (Hzn)) are composed of resedimented glaciolacustrine varves. Also shown in the images are the varve number of the couplet immediately overlying a landslide deposit of the event horizons (e.g., V1325 in E), the sand bed in Core LkDass15-04 (B), and varve 1528 (C), which is a regionally distinctive varve in the Timiskaming varve series. Note, in B), the more dense sand bed appears white in the radiograph image that was photo-edited to show the details of the varve couplets. Also, the mottled sediment immediately overlying the sand bed is likely sloughed debris from the sidewall rather than *in situ* sediment, as it sits at the very top of the core segment.**

A bed of rhythmic laminations, 0.14 m thick, directly overlies the landslide deposit of horizon B in core LkDass15-04 (Fig. 6A). The basal contact is sharp in the radiographs, but indistinct in the split cores. The lower ~ 20 mm of the bed is composed of three couplets, 5 to 9 mm thick, that are overlain by multiple, deformed couplets, up to several millimetres thick (Fig. 6A). It is unclear if the couplets are varves. Identified as a transitional glaciolacustrine-lacustrine deposit in Fig. 5, the couplet bed may be equivalent to the gray silt deposit, described by Stroup et al. (2013), which underlies lacustrine deposits in a number of modern lake basins that were also previously inundated by glacial Lake Ojibway. Basal contact of the overlying lacustrine deposits with the couplet bed is sharp and irregular with colour changes observed between the lower to higher deposits.

## 6. VARVE THICKNESS RECORD

The thicknesses of 546 measured varves of a composite sequence from the six cores are plotted in Fig. 7 (also see Brooks, 2016a). Stratigraphically, the recovered sequence is continuous, except where interrupted by the landslide deposits of event horizons E and H and by a zone of strong microfaulting, ~50 mm thick, in the lowest segment of core LkDass15-02. In Fig. 7, the Dasserat varve thickness record is shown with those from lakes Duparquet and Montbeillard (Breckenridge et al., 2012) and, A7, B7-B8a, and F5-F6-F7-F8 from the Timiskaming varve series (Antevs, 1925, 1928). The correlation of the portion of the Dasserat record above horizon E to the Timiskaming varve series is based on the presence of varve 1528, a regionally distinctive varve that marks a significant increase in varve thickness (Figs. 6C and 7; Antevs, 1925, 1928; Hughes, 1965). Antevs varve numbers 1484 to 1637 are thus assigned in sequence to the measured varves above and below varve 1528. An additional 13 varve numbers (to varve 1650) are assigned to varves that were too thin and/or deformed to be measured; these are not included in Fig. 7. Varve numbers 1039 to 1435 are assigned to varves below horizon E, based on similar thickness patterns to the Duparquet and Montbeillard records. Correlation to the other varve records, revealed an unconformity of 48 ‘missing’ varves below horizon E (Fig. 7).

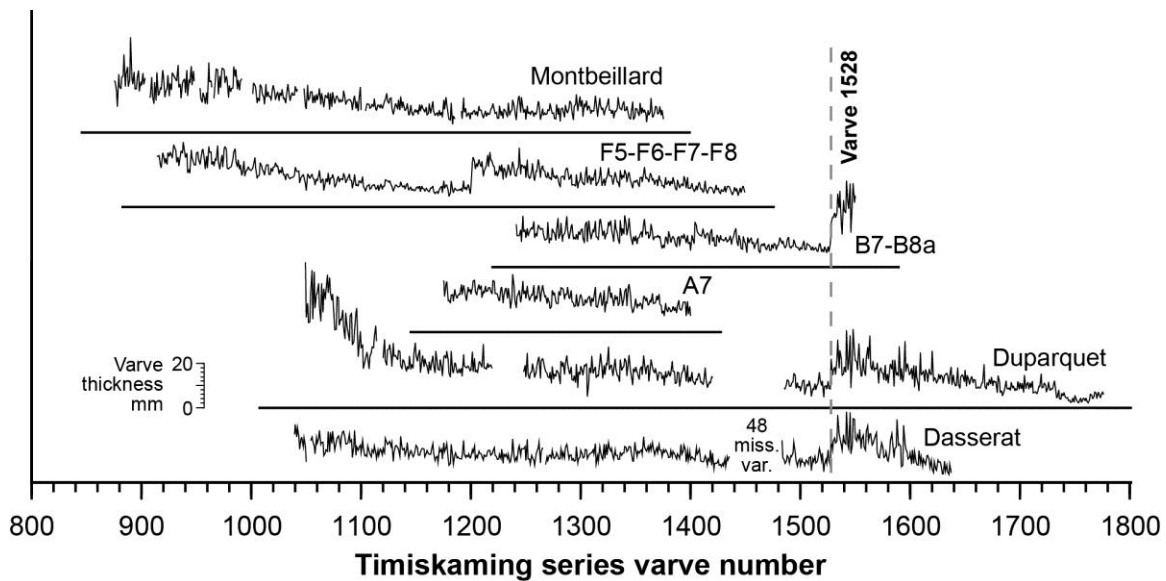


**Figure 7: Plots of the varve thickness versus numbering for the Dasserat varve record as well as for lakes Duparquet and Montbeillard, and the Timiskaming A7, B7-B8a, and F5-F6-F7-F8 records (data courtesy of A. Breckenridge; see Table 2 for correlation statistics between the Dasserat and three Timiskaming records). Note, the marked increase in varve thickness at varve 1528 within the Dasserat, Duparquet, and B7-B8a plots.**

Cross-correlation statistics from ANTEVS (V1.1) varve correlation software (Vollmer, 2014) between the Dasserat and the Timiskaming A7, B7-B8a, and F5-F6-F7-F8 varve records are listed in Table 2. Pearson’s  $r$  values of 0.499 to 0.609 at offsets of zero years are interpreted to support the varve numbering assigned to the Dasserat record shown in Fig. 7 (Rayburn and Vollmer, 2013). Possible error in the numbering of the Dasserat varve record relative to the three Timiskaming varve records is estimated to be  $\pm 2$  varve numbers, based on shifts of one

to two varves in the positions of distinctive peaks and troughs. These shifts are localized between the records and may reflect missing and false varves that self-cancel up and down the records (Lamoureux, 2001).

**Table 2: Cross-correlation statistics of the Dasserat varve record (1039-1637) compared to selected records of the Timiskaming varve series (see Fig. 7 for plots of the records).**

Varve series	$r^a$	$z^b$	$n^c$	$t^d$	Offset
Timiskaming A7	0.574	4.544	226	8.612	0
Timiskaming B7-B8a <sup>e</sup>	0.499	4.841	310	8.764	0
Timiskaming F5-F6-F7-F8	0.609	5.504	398	12.135	0

- <sup>a</sup>     Pearsons' r values
- <sup>b</sup>     z –score
- <sup>c</sup>     Number of overlapping varves
- <sup>d</sup>     Significance measurement
- <sup>e</sup>     Record includes varve 1528

## 6.1 EVENT HORIZON VARVE AGES

The interpreted varve ages of the event horizons are listed in Table 3 and plotted on Fig. 8. The ages of horizons H, G, F, and E are interpreted from the varve number of the partial or complete couplet immediately overlying the respective landslide deposit. This assumes that varve formation was re-established within the same or following year after the failure for the partial or complete varve, respectively.

The varve age of horizon E is derived from cores LkDass15-01, -03, -05, and -07, each of which penetrated separate landslide deposits within the horizon and contain overlying varves (Figs. 2 and 5). The youngest overlying varve is 1484 in three of these cores, and 1485 in the fourth (Fig. 5). The age of horizon E is thus interpreted to be varve year (vyr) 1483, but it is possible that at least one failure occurred during the following year. The consistency of the varve ages from these four cores supports the assumption that the varve number of the youngest overlying varve is representative of the landslide deposit age and thus avoids using underlying varves that may be truncated by an erosional unconformity.

**Table 3: Interpreted varve ages and inferred radiocarbon ages for the Lac Dasserat event horizons.**

Event horizon	Varve year (Timiskaming varve series) <sup>a</sup>	Age (cal yr BP) <sup>b</sup>	Comment
A	between 1650 and ~2100	between 8920 ± 200 and 8470 ± 200	– Maximum age is based on youngest identified varve in Dasserat varve record. Minimum age is based on final drainage of glacial Lake Ojibway.
B	between 1650 and ~2100	between 8920 ± 200 and 8470 ± 200	– As above.
C	between 1650 and ~2100	between 8920 ± 200 and 8470 ± 200	– As above.
D	between 1484 and 1637	between 9086 ± 200 and 8933 ± 200	– Age range is based on the varve immediately overlying horizon E and the youngest measured varve in the Dasserat varve record.
E	1483 <sup>c</sup>	9087 ± 200 <sup>c</sup>	– Varve age of horizon E is interpreted from core recovered from four sites: youngest varve overlying horizon E is 1484 in three of four cores, and youngest varve in the fourth core is 1485.
F	1364 <sup>c</sup>	9206 ± 200 <sup>c</sup>	– Varve age is interpreted from a single core.
G	1324 <sup>c</sup>	9246 ± 200 <sup>c</sup>	– Varves overlying horizon G were sampled in two cores. Youngest varve overlying horizon G is 1325 in one core and 1330 in the other. Interpreted age is based on the younger overlying varve, as explained in the text.
H	1267 <sup>c</sup>	9303 ± 200 <sup>c</sup>	– Varve age is consistent between two cores that penetrated the same landslide deposit.

<sup>a</sup> In the Timiskaming varve series, the varves are numbered from oldest to youngest beginning at varve number one.

<sup>b</sup> Calibrated ages and uncertainty ranges are derived by subtracting a given horizon varve age from 2100 (approximately youngest varve number in the Timiskaming varve series), then adding the difference to 8470 ± 200 cal yr BP. The latter age is the estimated radiocarbon age for the demise of glacial Lake Ojibway (after Breckenridge et al. 2012). All of the age uncertainty is associated with the radiocarbon age.

<sup>c</sup> Age is interpreted from the varve number of the youngest complete varve (less one year) or partial varve overlying the respective landslide deposit.

Based on a single core (LkDass15-03), the youngest varve overlying horizon F is 1365 (Figs. 5 and 6D), indicating that this landslide failed in yr 1364. Varves 1325 and 1330 contained in

cores LkDass15-07 and -05, respectively, are the youngest varves overlying horizon G (Figs. 5, 6E and 6F). Located on physically separate deposits in the northeast and south basins, the varve numbers indicate that the landslides were emplaced in *vyr* 1324 and 1329, and thus seem to represent temporally close, but separate failure events. Varve 1330 in core LkDass15-05, however, is immediately underlain by a disturbed bed, 20 mm thick, that in turn overlies two, possibly *in situ* varves situated upon a thick landslide bed (Fig. 6F). It is plausible that the thin disturbed bed underlying varve 1330 is a minor, secondary landslide bed and that the main horizon G landslide is the lower, thick deposit. Based on the younger overlying varve from core LkDass15-07, the age of horizon G is interpreted to be *vyr* 1324.

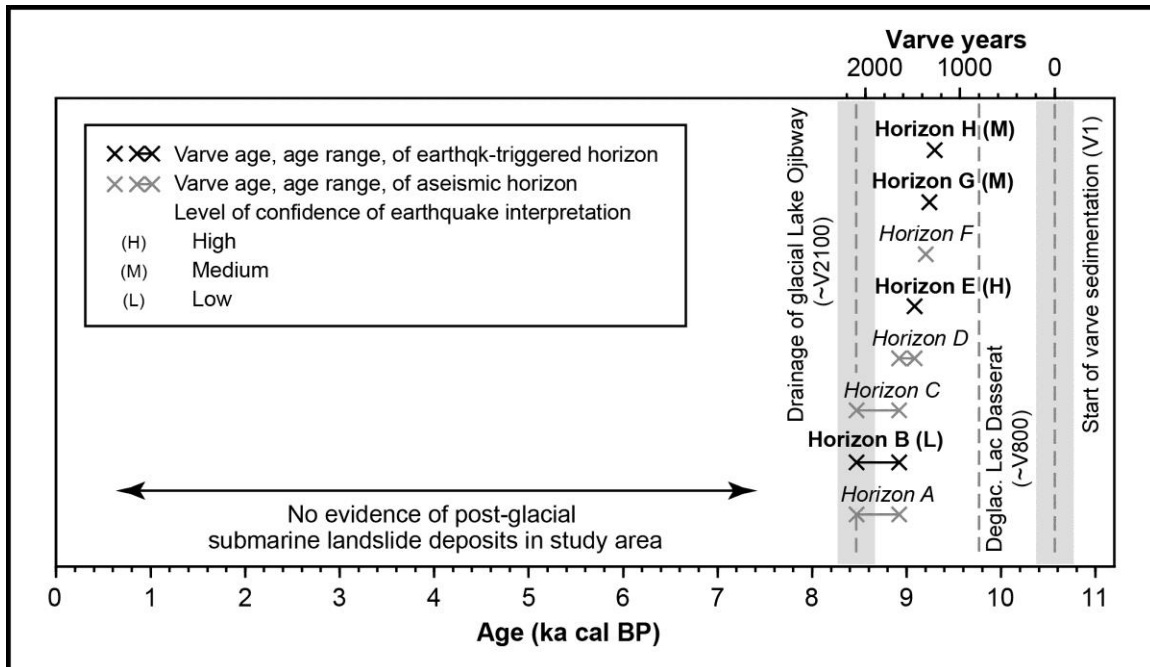


**Figure 8: Plot of the varve ages (or age ranges) of the event horizons superimposed over a timescale that spans varve sedimentation in glacial Lake Ojibway and the post-glacial lake period. The duration of glacial Lake Ojibway varve sedimentation is ~2100 *vyr*, ending at the drainage of the lake. Breckenridge et al. (2012) dated tentatively this interval as  $10,570 \pm 200$  to  $8470 \pm 200$  cal yr BP; the shaded areas on the figure represent the  $1\sigma$  ranges associated with these calibrated radiocarbon ages. Also shown is the estimated time of deglaciation of the Lac Dasserat area (~*vyr* 800 (or about  $9770 \pm 200$  cal yr BP)) that marks the approximate start of local varve sedimentation at the study area (Breckenridge et al., 2012, their Fig. 7). The span of the interpreted paleoearthquakes is up to 834 *vyr*, and may represent a concentration of elevated seismicity that occurred during the late glacial interval, as mentioned in the text.**

Two closely-spaced cores; LkDass15-01 and -02, penetrated extensions of the same landslide deposit of horizon H. The youngest measured varve in each core is 1268 (Fig. 5 and 6G), indicating the landslide failed in *vyr* 1267, which is inferred to represent the age of horizon H. The long sequence of varves beneath horizon H in core LkDass15-02 does not imply an absence of event horizons through *vyr* 1039-1266 within the study area (Fig. 5), as this core did not targeted deeper, unmapped landslide deposits (Fig. 3). There is strong microfracturing

within varves 1051-1053 (Fig. 5), but it is not apparent from the profile returns if this interval corresponds to an unmapped landslide deposit.

The ages of horizons D, C, B, and A are estimated only broadly (Table 3; Fig. 8). Horizon D is interbedded within the varve deposits, but was not penetrated by any of the cores. Its age is between *vyr* 1484 and 1637, based on its stratigraphic position in the profile returns between the youngest varve overlying horizon E and the oldest, measured varve near the top of the varve sequence (Fig. 3C). Horizons C, B, and A are not interbedded within the varve deposits and no core recovered deposits of horizons C and A. However, a maximum age of *vyr* 1650 is assigned to these horizons, based on the youngest counted (not measured) varve in the varve sequence underlying horizon B (Fig. 5 and 6B). Assuming horizons C, B, and A do not post-date the final drainage of glacial Lake Ojibway, a minimum age for these horizons is *vyr* ~2100, based on the youngest varve in the Timiskaming varve series.

## 7. DISCUSSION

Previous studies have interpreted the occurrence of multi-landslide event horizons as evidence of paleoearthquakes, based on analogous landslide signatures from historical earthquakes (Schnellman et al., 2002, 2006; Strasser et al., 2006). By extension, the strong and moderately-strong multi-landslide signatures of horizons E and B, and H and G, respectively, each could be evidence of a paleoearthquake in the Lac Dasserat area. This inference is circumstantial, however, without a historical analogue because the study area is located outside of the Western Quebec Seismic Zone (Fig. 1). Also, three horizons (H, G, and E) accumulated within glacial Lake Ojibway and the fourth (horizon B) during the transition from a glacial to postglacial lake; both of these depositional settings represent different environments from that of post-glacial Lac Dasserat, which lacks landslide deposits within the study area (Fig. 3). Thus the interpretations of the triggering mechanisms of these horizons need to consider aseismic causes that are consistent with the environmental settings at the time of formation rather than simply assuming a paleoearthquake trigger (Jibson, 2009; Owen et al., 2011; Sims, 2012).

With respect to the glacial lake setting, four reasonable aseismic mechanisms for the formation of horizons H, G, and E are assessed in Table 4, based on current understanding of the dynamics of glacial Lake Ojibway. The assessments assume a deep water, distal depositional environment; deep water is inferred because clay-silt varves in glacial Lake Ojibway formed in depths in excess of 30 to 50 m (Hughes, 1959; Veillette, 1983, 1994). The temporal context is the interval of aggradation of the Dasserat varve series (*vyr* 1039 to 1650), when the ice front ranged from 40 km to greater than 200 km north of the Lac Dasserat (Breckenridge et al., 2012, their Fig. 7). Of the identified mechanisms, grounded icebergs and oversteepening/overloading of slopes could account for isolated failures in the study area, but both seem unlikely to explain the occurrences and lateral extent of the multi-landslide horizons (Table 4). In particular, the near-absence of ice-rafted debris in the varve deposits implies that few icebergs were in the study area during the interval of interest. Also, horizons H, G, and E pre-date *vyr* 1528 when there was a marked increase in varve sedimentation regionally within the glacial lake (Fig. 6C); there is no multi-landslide horizon post-*vyr* 1528 that could be attributed to this increase. Both wind-generated waves and rapid drawdown of the lake level also are considered to be unlikely mechanisms. While undoubtedly there were significant wind storms on glacial Lake Ojibway, the influence of wave action on the lake bed would be limited over the study area in (what was then) deep water conditions. Although waves possibly could have generated failures along eroding shorelines, the closest paleoshoreline to the study area was ~1.5 km away (Table 4). There are no known rapid draw-down events of glacial Lake Ojibway during the time interval of interest, negating an otherwise viable mechanism.

**Table 4: Assessment of possible aseismic mechanisms in glacial Lake Ojibway for event horizons H, G, and E.**

Mechanism	Comments	Assessment
Grounding icebergs	<ul style="list-style-type: none"> <li>– Could mechanically trigger failures from higher surfaces of lake bottom.</li> <li>– Iceberg scour marks are present on bed of glacial Lake Ojibway, but are located over 90 km north of the study area (Dionne, 1977; Veillette and Paradis, 1996).</li> <li>– Near absence of ice-rafted debris in varve deposits in study area implies that few icebergs were present during interval of Dasserat varve record.</li> </ul>	May have caused isolated failures in study area, but unlikely to account for the multi-landslide signatures of horizons H, G, and E.
Overloading or oversteepening of slopes	<ul style="list-style-type: none"> <li>– Failures could result from high sedimentation rates on the undulating slopes within general location of study area.</li> <li>– Depositional setting is in deep water and distal with respect to sediment source implying that there are no pockets of high localized sedimentation in study area.</li> <li>– Difficult to account for the shift in the locations of failures between horizons H and G, and then the widespread failures occurring in horizon E, with this mechanism.</li> <li>– An obvious increase in the regional sedimentation rate occurred in the glacial lake beginning at varve 1528, but this change post-dates horizons H, G, and E and there is no multi-landslide horizon in the study area until after varve sedimentation began to wane (horizon B).</li> </ul>	May have caused isolated failures in study area, but unlikely to account for the multi-landslide signatures of horizons H, G, and E.
Wind-generated waves	<ul style="list-style-type: none"> <li>– Storms on glacial Lake Ojibway generated large waves during the interval of Dasserat varve record.</li> <li>– Deep water conditions (minimum 30 to 50 m deep) over study area probably minimized influence of wave actions on lake bed.</li> <li>– Waves might have triggered failures along an eroding shoreline, however, the nearest paleoshoreline in relevant period was located ~1.5 km to the south-southwest along the northeastern tip of a narrow, elevated bedrock ridge.</li> <li>– If wind-generated waves are an important mechanism, then there should be a greater number of event horizons with a relatively low rather than high number of landslide deposits, reflecting the higher frequency of lower magnitude storm events, but this opposite to what is observed.</li> <li>– Periods of 40 to 119 varve years between horizons H, G, F and E without any failures in study area further suggest this is not an important mechanism because significant storms almost certainly occurred more frequently than the duration of these periods.</li> </ul>	Unlikely to account for the multi-landslide signatures of horizons H, G, and E.
Rapid drawdown of lake level	<ul style="list-style-type: none"> <li>– Could trigger failures due to generation of high pore pressure in poorly-draining, clay-silt deposits and loss of stabilizing influence of water pressure on slopes.</li> <li>– No known rapid drawdown events of glacial Lake Ojibway during interval of Dasserat varve record.</li> </ul>	Unlikely to account for the multi-landslide signatures of horizons H, G, and E.

**Table 5: Listing of youngest varve overlying disturbed glaciolacustrine deposits at sites in region, as reported in literature. See Fig. 9 for map of locations.**

Varve measurement site	Site description (as worded in original source)	Longitude	Latitude	Number of youngest overlying varve	Comments
Antevs' site 123	Slide on E side of Abitibi River, 5.5 km NW of Iroquois Falls, Ontario.	-80.75 <sup>a</sup>	48.83 <sup>a</sup>	1486	<ul style="list-style-type: none"> <li>– First reported varve overlying “5 ft contorted clay to river level” (Antevs, 1928).</li> <li>– Interpreted minimum varve age of contorted clay is 1485.</li> <li>– Contorted clay inferred to be equivalent to Dasserat horizon E.</li> </ul>
Antevs' site 128	Slide on the E side of Frederick House River just below falls.	-81.017 <sup>b</sup>	48.793 <sup>b</sup>	1485 or 1487	<ul style="list-style-type: none"> <li>– First reported varve overlying “5 ft silt in disturbed thick varves” (Antevs, 1928).</li> <li>– There is an inconsistency in the site summary about whether the measured varve sequence starts at 1485 or 1487.</li> <li>– Interpreted minimum varve age of disturbed thick varves is 1484 or 1486.</li> <li>– Disturbed zone inferred to be equivalent to Dasserat horizon E.</li> </ul>
Antevs' site 134	Located ~2 mi of locality 128 and 150 yd S of the new river channel, slide on the W side of the [Frederick House] river.	-81.026 <sup>b</sup>	48.801 <sup>b</sup>	1484	<ul style="list-style-type: none"> <li>– First reported varve overlying “12 ft partly disturbed varved silt, probably about 70 varves” (Antevs, 1928).</li> <li>– Interpreted minimum varve age of disturbed varved silt is 1483.</li> <li>– Disturbed varves inferred to be equivalent to Dasserat horizon E.</li> </ul>
Antevs' site 135	150 yd N of locality 134, the E side of the new river channel [along the Frederick House river].	-81.030 <sup>b</sup>	48.803 <sup>b</sup>	1488	<ul style="list-style-type: none"> <li>– First reported varve overlying “15 ft clay and silt partly disturbed and covered to river level” (Antevs, 1928).</li> <li>– Interpreted minimum varve age of disturbed sediments is 1487.</li> <li>– Disturbed sediments inferred to be equivalent to Dasserat horizon E.</li> </ul>
Antevs' site 91	2.75 mi SE of Matheson, 1 mi SSE of Belleek, bluff on the W side of Black River at the	-80.418 <sup>c</sup>	48.513 <sup>c</sup>	1486	<ul style="list-style-type: none"> <li>– First reported varve overlying “disturbed zone” (Antevs, 1925).</li> <li>– Interpreted minimum varve age of disturbed</li> </ul>

	river bend E of the railway				zone is 1485.
Antevs' site 85	7 mi SE of Matheson, 2.25 mi SE of Vimy Ridge, bluff on the tributary from the SW to the Black River, on the W side 200 yd S of the mouth.	-80.3519 <sup>b</sup>	48.4745 <sup>b</sup>	1490	<ul style="list-style-type: none"> <li>- Disturbed zone inferred to be equivalent to Dasserat horizon E.</li> <li>- First reported varve overlying "3 ft contorted clay-sand and very fat and, yellow clay kneaded together" (Antevs, 1925).</li> <li>- Interpreted minimum varve age of contorted clay-sand is 1489.</li> <li>- Contorted clay-sand inferred to be equivalent to Dasserat horizon E.</li> </ul>
Hughes' Ghost River 1 section	Site on N and S sides of Hwy 101, 0.6 mi east of Ghost River on the E side of a small NW-flowing tributary of Ghost River.	-79.8584 <sup>d</sup>	48.5292 <sup>d</sup>	1486	<ul style="list-style-type: none"> <li>- First reported varve overlying "varved clay, disturbed" (Hughes, 1959).</li> <li>- Interpreted minimum varve age of varved clay, disturbed is 1485.</li> <li>- Disturbed clay inferred to be equivalent to Dasserat horizon E.</li> </ul>
Hughes' Twin Falls section	Site on E side of Abitibi River, about 150 yd downstream of E abutment of Twin Falls dam.	-80.5787 <sup>d</sup>	48.7442 <sup>d</sup>	1485	<ul style="list-style-type: none"> <li>- First reported varve overlying "varved clay, disturbed (varves 1456 to 1484 missing)" (Hughes, 1959).</li> <li>- Interpreted minimum varve age of varved clay, disturbed is 1484.</li> <li>- Disturbed clay inferred to be equivalent to Dasserat horizon E.</li> </ul>
Lac Duparquet coring site DQ09-2A	Coring site on Lac Duparquet located approximately 5.6 km WNW of public boat launch at Duparquet, QC.	-79.3013 <sup>c</sup>	48.50925 <sup>c</sup>	1485	<ul style="list-style-type: none"> <li>- First varve overlying bed of deformed varves about 1.2 m thick (from Breckenridge et al., (2012) and A. Breckenridge, unpublished data).</li> <li>- Interpreted minimum varve age of deformed varves is 1484.</li> <li>- Deformed varves inferred to be equivalent to Dasserat horizon E.</li> </ul>
Antevs' site 89	300 yd E of location 88, which is described as, 6.5 mi ESE of Matheson, bluff on the south side of Pike River, 700 yd W of bridge, at the sharp bend of the river towards the west.	-80.320 <sup>c</sup>	48.515 <sup>c</sup>	1324	<ul style="list-style-type: none"> <li>- First varve underlying "disturbed clay" (Antevs, 1925).</li> <li>- Interpreted minimum varve age of disturbed clay is 1325.</li> <li>- Disturbed clay inferred to be equivalent to Dasserat horizon G.</li> </ul>
Antevs' site 86	5.25 mi SE of Matheson, 0.75 mi SE of Vimy Ridge,	-80.3761 <sup>e</sup>	48.4857 <sup>e</sup>	1326	<ul style="list-style-type: none"> <li>- First (?) varve overlying "3 ft faulted clay" (Antevs, 1925).</li> </ul>

	roadcut on the E side of the railway, at the brook.				<ul style="list-style-type: none"> <li>– Interpreted minimum varve age of faulted clay is 1325.</li> <li>– Faulted clay inferred to be equivalent to Dasserat horizon G.</li> </ul>
Antevs' site 116	Slide along W side of Abitibi River	-79.297 <sup>b</sup>	48.595 <sup>b</sup>	1264	<ul style="list-style-type: none"> <li>– First(?) varve overlying "slidden zone, 4 inches thick that represents 2 varves" (Antevs, 1928).</li> <li>– Interpreted minimum varve age of slidden zone is 1263.</li> <li>– Slidden zone inferred to be equivalent to Dasserat horizon H.</li> </ul>

---

<sup>a</sup> Geographical coordinates from Antevs (1928).

<sup>b</sup> Geographical coordinates derived from Google Earth, based on site description and map in Antevs (1928).

<sup>c</sup> Geographical coordinates from Breckenridge et al. (2012).

<sup>d</sup> Geographical coordinates derived from Google Earth, based on descriptions in Hughes (1959).

<sup>e</sup> Geographical coordinates derived from Google Earth, based on site description and map in Antevs (1925).

The lack of credible aseismic mechanisms implies that paleoearthquakes are the best explanation for event horizons H, G, and E, and there is independent evidence to support this premise. In summary logs of the varve measurement sites examined in the Timmins-Lac Abitibi region, Ontario-Quebec, Antevs (1925, 1928) and Hughes (1959) recorded the presence of “contorted”, “deformed”, “disturbed” or “slidden” varve zones (referred to as disturbed varves hereafter) interbedded within sequences of numbered varves of the Timiskaming varve series. The varve number (less one year) of the youngest couplet in the overlying varve sequence provides a minimum varve age for the disturbed deposit. In addition, Breckenridge et al. (2012, their Fig. 5) report the presence of deformed varves in a core collected from Lac Duparquet, and Adams (1982) mentions zones of contorted varves being present at a number of locations within a triangular region between Macamic and Ville Marie, Quebec, and Porcupine, Ontario.

As summarized in Table 5, the data from Antevs (1925, 1928), Hughes (1959) and Breckenridge et al. (2012) reveal that disturbed deposits with minimum ages of vyr 1483-1489, vyr 1325, and vyr 1263 are present at nine, two, and one sites located 32 to 135 km from the study area (Fig. 9). Similarly, the best-developed synchronous deformation observed by Adams (1982) happened in vyr 1487. Although his site locations are only shown on a crude map (Adams, 1989, his Fig. 5), many evidently are near those of Antevs (1925, 1928) and Hughes (1959). Because of the tight chronological control provided by the Timiskaming varve series, it is inferred that these reported disturbed deposits are synchronous with the nearly identical varve ages of Dasserat horizons E (vyr 1483), G (vyr 1324) or H (vyr 1267) and that each group is the product of a common regional trigger. The occurrence of paleoearthquakes readily accounts for the commonly-aged landslide/disturbed deposits at the widely-spaced locations, especially in the case of the numerous sites of the vyr 1483-1489 group. Following the qualitative concept of Moneke et al. (2006) and Strasser et al. (2013), the interpretative confidence that paleoearthquakes triggered horizons E, G, and H is high, medium and medium, respectively, for the reasons summarized in Table 6. The paleoearthquake interpretation for horizon E (1483-1489 group) is consistent with Adams' (1982) attribution of the occurrence of the aforementioned synchronous contortions in vyr 1487 to earthquake shaking.

Identifying the triggering mechanism of horizon B is more difficult than horizons H, G, and E because of the broadly defined chronology for horizon B (Fig. 8, Table 3) and possibly more complex depositional conditions. As noted, aggradation of horizon B occurred stratigraphically during the transition from a glacial to post-glacial lake (Figs. 3 and 5). Varve thicknesses decrease over the upper 0.5 m of the underlying varve deposits (post vyr 1600), especially over the upper 0.15 m, presumably reflecting decreasing water levels over the study area. The 0.08-m-thick, very fine sand bed that is interbedded between the top of the varve sequence and the overlying landslide deposit in core LkDass15-04 may be significant to interpreting horizon B (Figs. 5 and 6B), although its definitive interpretation is beyond the scope of this paper. The bed may correlate to a whitish silt bed reported by Daubois et al. (2015) that is situated at the top of the glaciolacustrine deposits and is commonly found within shallow glaciolacustrine exposures in the La Sarre, Quebec, and eastern Lac Abitibi areas (Fig. 9). Daubois et al. (2015) hypothesize that this silt bed formed during the final drainage of glacial Lake Ojibway. If both the correlation of these two beds and the drainage hypothesis are correct, the landslide deposits of horizon B may be draw-down failures.

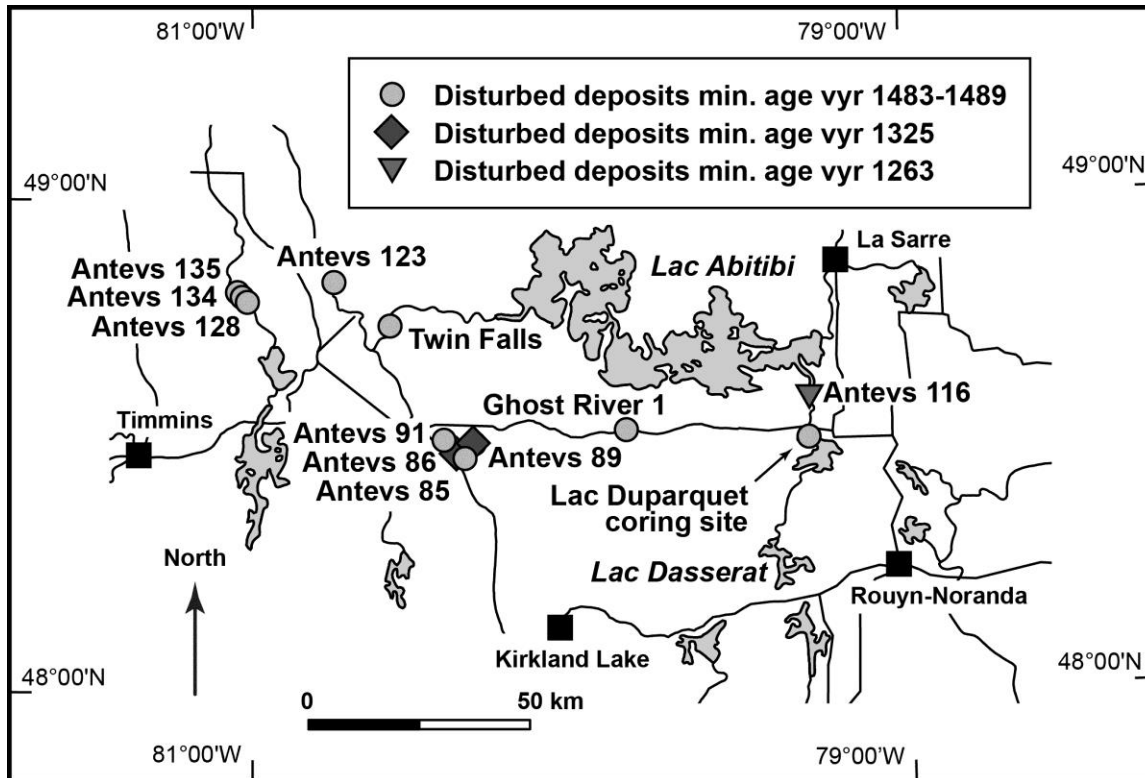


**Figure 9: Map showing the locations of varve sampling sites of Antevs (1925, 1928), Hughes (1959), and Breckenridge et al. (2012) where the varve ages of disturbed deposits are essentially identical to Dasserat event horizons H, G, or E, as mentioned in the text. The ages (or age ranges) shown in the legend are derived from the varve number (less one year) of the youngest undisturbed varve overlying a disturbed deposits that is mentioned in site descriptions - see Table 5s for summaries of these sites.**

Two factors, however, seem inconsistent with the above explanation. The Dasserat sand bed seems significantly older than the  $\text{vyr} \sim 2100$  age of the final drainage of glacial Lake Ojibway, since the bed is located only 0.1 m above varve 1650 in core LkDass15-04 and there is no obvious major underlying unconformity apparent in the profiling returns. No older draw-down events have been identified for glacial Lake Ojibway that might explain this bed. More significantly, the source area of one of the failures is clearly located below the modern level of Lac Dasserat (failure 13 in Figs. 3C and 4B), which seems inconsistent with a draw-down mechanism. Alternatively, the similarity of the strong multi-landslide signatures of horizons B and E may be supportive of a paleoseismic trigger. Landslide deposits at the glaciolacustrine-lacustrine interface are also present in other lakes in the Rouyn-Noranda area, including lakes Opasatica, Duparquet, Dufresnoy, and Joannès (Brooks, 2016b; Brooks, unpublished data), although this is definitive of neither a seismic or draw-down mechanism.

**Table 6: Qualitative levels of interpretative confidence that event horizons E, G, H, and B within Lac Dasserat were triggered by paleoearthquakes.**

Event horizon (varve year)	Level of interpretative confidence	Rationale
E (1483)	High	<ul style="list-style-type: none"> <li>- strong multi-landslide signature.</li> <li>- multiple occurrences of disturbed deposits with similar age in region.</li> <li>- no aseismic process represents a reasonable alternative explanation (see Supplementary Table 1).</li> </ul>
G (1324)	Medium	<ul style="list-style-type: none"> <li>- moderately-strong multi-landslide signature.</li> <li>- two occurrences of disturbed deposits with similar age in region.</li> <li>- no aseismic process represents a reasonable alternative explanation (see Supplementary Table 1).</li> </ul>
H (1267)	Medium	<ul style="list-style-type: none"> <li>- moderately-strong multi-landslide signature.</li> <li>- one occurrence of disturbed deposits with similar age in region.</li> <li>- no aseismic process represents a reasonable alternative explanation (see Supplementary Table 1).</li> </ul>
B (1650 to ~2100)	Low	<ul style="list-style-type: none"> <li>- strong multi-landslide signature.</li> <li>- rapid draw-down is a possible alternative aseismic trigger, if very fine sand bed that underlies horizon B in core LkDass15-04 is evidence of an unrecognized pre-vyr 2100 drainage event of glacial Lake Ojibway.</li> <li>- the depth location of the source area of one failure in horizon B is beneath surface of modern Lac Dasserat, which seems inconsistent with a draw-down mechanism.</li> </ul>

While currently available data preclude a definitive interpretation of the triggering mechanism for horizon B, on balance they seem supportive a paleoseismic origin, based on the combination of a strong multi-landslide signature, the occurrence of a failure source area below the modern level of Lac Dasserat, and the lack of a known pre-vyr 2100 draw-down event (Table 6). Weighing this evidence, the interpretative confidence that horizon B is the product of a paleoearthquakes, however, is considered low (Table 6). This interpretation needs re-evaluation as new data becomes available relating to, for example, the age and origin of the Dasserat sand bed, a better defined age for horizon B, and the possible occurrence of a pre-vyr 2100 draw-down event(s) of glacial Lake Ojibway.

The single and paired landslide signatures of horizons F, D, C, and A are not considered to be evidence of paleoseismicity, based on available data, as they could reasonably be explained by an aseismic mechanism (Table 4). No disturbed deposits are reported by Antevs (1925, 1928) or Hughes (1959) that correlate to the varve age of horizon F (vyr 1364). Their results cannot be compared directly to horizons D, C, and A whose ages are wide varve ranges (Table 3). The non-paleoseismic interpretation attributed to the single landslide deposit of horizon F is notable because it is the most extensive and thickest in the study area. Similarly, Schnellmann

et al. (2002) also interpreted that a large, stratigraphically-isolated landslide of postglacial age in Lake Lucerne, Switzerland, was not evidence of a paleoearthquake.

The interpreted paleoearthquakes that triggered the multiple landslides of horizons H, G, E, and B had minimum shaking intensities of VI to VII (Michetti et al., 2015); at these levels, multiple landslides become common. It is premature to make more refined estimates until the regional extent of the landslide signatures of each paleoearthquake is better known. Based on the overall evidence, the paleoearthquake that formed horizon E at approximately  $\text{vyr } 1483$  seems to have been the largest event because of its apparent broad regional signature (Fig. 9). Adams (1982) estimated that the magnitude of this earthquake was  $\geq M 5.7$ . The locations of the paleoearthquake epicentres or causative faults are unknown, but can be estimated from the central areas of the regional patterns of the landslide signatures as these become established, as done provisionally by Adams (1989, his Fig. 5).

The stratigraphic position and varve ages of horizons H, G, E, and B reveal that the interpreted paleoearthquakes occurred during regional deglaciation between  $\text{vyr } \sim 800$  and  $2100$  ( $9770 \pm 200$  and  $8470 \pm 200$  cal yr BP), when glacial Lake Ojibway inundated the Lac Dasserat area (Fig. 8, Table 3). The horizon varve ages further reveal that the four interpreted paleoearthquakes occurred at intervals of 58 and 160  $\text{vyr}$ , and up to 618  $\text{vyr}$ ; the latter interval is based on the minimum varve age for horizon B ( $\text{vyr } 2100$ ; Table 3). These intervals span up to 834  $\text{vyr}$ , which represents  $\sim 10\%$  of the post-glacial Lake Ojibway timespan and defines a temporal concentration of seismicity during regional deglaciation (Fig. 8). Some of the unmapped deeper landslide deposits in Lac Dasserat may be evidence of additional paleoearthquakes that happened in the earlier stage of local deglaciation between  $\text{vyr } 800$  and  $1266$  (Figs. 3 and 8).

The lack of landslide signatures within the postglacial lacustrine deposits of the study area may indicate that shaking locally has not exceeded intensities of VI to VII since the demise of glacial Lake Ojibway (i.e., post  $\sim 8470 \pm 200$  cal yr BP). Such a conclusion is premature, however, since unrecognized post-glacial, seismogenic landslide deposits (or other evidence of paleoseismicity) may exist within the Dasserat basin or in another area lake basins. Nevertheless, the interpretation of four (or even three) paleoearthquakes at the time of glacial Lake Ojibway, plus the possibility of additional evidence of paleoseismicity from older, unmapped submarine landslides in the study area, is consistent with elevated seismicity during deglaciation. If correct, then the interpreted paleoearthquakes identified in this study represent a Canadian example of elevated seismicity associated with relatively rapid crustal unloading during deglaciation that occurred within an area of low historical seismicity (Fig. 1A).

## 8. CONCLUSIONS

This study demonstrates the application of an integrated seismo- and chrono-stratigraphic approach to investigate evidence of paleoseismicity preserved in late glacial deposits within a lake basin of eastern Canada. The landslide deposits used to define the event horizons could all be mapped exclusively from the profiling returns, which would have identified the multi-landslide signatures. However, it was only through recovering core that the crucial chronological data was obtained that allowed three of the four multi-landslide horizons to be correlated to disturbed varve deposits mentioned in the regional literature, thereby helping corroborate the paleoearthquake interpretations.

Landslide deposits form a significant portion of the sub-bottom of the Lac Dasserat study area. The majority of the 74 mapped deposits fall within four event horizons. Horizons E and B

exhibit strong multi-landslide signatures, while the signatures of horizons H and G are moderately strong. The single and paired deposits of horizons D, C, and A represent minor landslide signatures. Older unmapped and undated landslide deposits are present within the lower part of the sub-bottom.

Horizons H, G, F, and E are interpreted to date to vyr 1267, 1324, 1364 and 1483, respectively, relative to the Timiskaming varve series. The other horizons are dated as ranges, with horizon D occurring between vyr 1484 and 1637, and horizons C, B, and A between vyr 1650 and ~2100.

Horizons E, G, and H are interpreted to be evidence of paleoearthquakes with high to medium levels of interpretative confidence. Horizon B is also interpreted to be evidence of a paleoearthquake, but with a low interpretative confidence because of the possibility that it was caused by an unrecognized drawdown of glacial Lake Ojibway. The single and paired landslide signatures of horizons F, D, C, and A are not considered to be evidence of paleoearthquakes, based on available data. The interpretations of all eight event horizons should be re-evaluated as new data becomes available on the age and location of submarine landslide deposits elsewhere in the region and, in the case of horizon B, also on the post-vyr 1650 dynamics of glacial Lake Ojibway.

The four interpreted paleoearthquakes occurred between vyr ~800 to 2100 ( $9770 \pm 200$  to  $8470 \pm 200$  cal yr BP) during regional deglaciation when glacial Lake Ojibway was impounded behind the Laurentide Ice Sheet. They may represent a period of elevated seismicity associated with crustal unloading arising from the retreat of the ice sheet that occurred within an area now experiencing low historical seismicity.

The identification of four paleoearthquakes and the possible period of elevated seismicity during deglaciation provide an interpretative framework that can be augmented and revised by future paleoseismic research in northwestern Quebec-northeastern Ontario. Additional work is needed to delineate the regional extent of the landslide signatures thus enabling estimates of paleoearthquake magnitudes and identifying approximate epicentre locations. Collectively, such research will contribute to greater understanding of long-term seismicity in this intracratonic setting.

## **Acknowledgements**

Comments from John Adams, Jim Hunter, Mike Lewis and Jean Veillette, and journal reviewers John Clague and Martitia Tuttle are sincerely appreciated. I am most gratefully to Alain Grenier (GSC) for assistance with the profiling survey and coring, André Pugin (GSC) for guidance interpreting the profiling results, Kevin Brewer (GSC) for assistance with the profiling and GPS equipment, and Aldo Katragjini for assistance compiling the event horizon maps. Advice and digital varve thickness data from Andy Breckenridge used in correlating the Dasserat varves to the Timiskaming varve series are sincerely appreciated. He also kindly provided unpublished mosaic images of cores from Lac Duparquet. I thank Sue Pullan and Sam Alpay for alerting me to the presence of submarine landslide deposits in reconnaissance sub-bottom profiles from Lac Dasserat. This research was supported by the Public Safety Geoscience Program, Earth Sciences Sector, Natural Resources Canada and the Nuclear Waste Management Organization. This paper represents ESS Contribution 20150417.



## References

- Adams, J., 1982. Deformed lake sediments record prehistoric earthquakes during the deglaciation of the Canadian Shield (abstract). EOS, Transactions, American Geophysical Union 63, 436.
- Adams, J., 1989. Postglacial faulting in eastern Canada: Nature, origin and seismic hazard implications. *Tectonophysics* 163, 323-331.
- Adams, J., 1996. Paleoseismology in Canada: A dozen years of progress. *Journal of Geophysical Research* 101, 6193–6207. <http://dx.doi.org/10.1029/95JB01817>.
- Adams J., Basham, P., 1989. The seismicity and seismotectonics of Canada east of the Cordillera. *Geoscience Canada* 16, 3-16.
- Adams J., Basham, P., 1991. The seismicity and seismotectonics of eastern Canada. In: Slemmons, D.B., Engdahl, E.R., Zoback, M.D., Blackwell, D.D. (Eds.), *Neotectonics of North America*. Geological Society of America, Decade Map, v. 1, pp. 261-276.
- Alpay, S. (Ed.), 2016. Multidisciplinary environmental science investigations surrounding the former Aldermac mine, Abitibi, Quebec: The Lac Dasserat study workshop summarized. Open File 7993, Geological Survey of Canada, Ottawa. doi:10.4095/297747
- Anselmetti, F.S., Ariztegui, D., De Batist, M., Catalina, G.A., C., Habertzettl, T., Niessen, F., Ohlendorf, C., Zolitschka, B., 2009. Environmental history of southern Patagonia unravelled by the seismic stratigraphy of Laguna Potrok Aike. *Sedimentology* 56, 873–892. <http://dx.doi.org/10.1111/j.1365-3091.2008.01002.x>.
- Antevs, E., 1925. Retreat of the last ice-sheet in eastern Canada. Memoir 146. Geological Survey of Canada, Ottawa.
- Antevs, E., 1928. The last glaciation with reference to the retreat in northeastern North America. American Geographical Society Research Series No. 17, New York.
- Barber, D.C., Dyke, A., Hillaire-Marcel, C., Jennings, A.E., Andrews, J.T., Kerwin, M.W., Bilodeau, G., McNeely, R., Southon, J., Morehead, M.D., Gagnon, J.M., 1999. Forcing of the cold event of 8,200 years ago by catastrophic drainage of Laurentide lakes. *Nature* 400, 344-348.
- Basham, P.W., Weichert, D.H., Anglin, F.M., Berry, M.J., 1982. New probabilistic strong ground motion maps of Canada: a compilation of earthquake source zones, methods and results. Open File 82-33. Earth Physics Branch, Ottawa.
- Beck, C., 2011. Lake sediments as late Quaternary paleoseismic archives: examples in the northwestern Alps and clues for earthquake-origin assessment of sedimentary disturbances. In: Audemard M., F.A., Michetti, A.M., McCalpin, J.P. (Eds.), *Geological criteria for evaluating seismicity revealed: forty years of paleoseismic investigations and the natural records of past earthquakes*. Geological Society of America, Special Papers 479, pp. 159–179. [http://dx.doi.org/10.1130/2011.2479\(07\)](http://dx.doi.org/10.1130/2011.2479(07)).

- Becker, A., Ferry, M., Monecke, K., Schnellmann, M., Giardini, D., 2005. Multiarchive paleoseismic record of late Pleistocene and Holocene strong earthquakes in Switzerland. *Tectonophysics* 400, 153-177.  
<http://dx.doi.org/10.1016/j.tecto.2005.03.001>.
- Bertrand, S., Charlet, F., Chapron, E., Fagel, N., De Batist, M., 2008. Reconstruction of the Holocene seismotectonic activity of the Southern Andes from seismites recorded in Lago Icalma, Chile, 39° S. *Palaeogeography, Palaeoclimatology, Palaeoecology* 259, pp. 301-322. <http://dx.doi.org/10.1016/j.palaeo.2007.10.013>.
- Breckenridge, A., Lowell, T.V., Stroup, J.S., Evans, G., 2012. A review and analysis of varve thickness records from glacial Lake Ojibway (Ontario and Quebec, Canada). *Quaternary International* 260, 43-54.
- Brooks, G.R., 2015. An integrated stratigraphic approach to investigating evidence of paleoearthquakes in lake deposits of eastern Canada. *Geoscience Canada* 42, 247-261.
- Brooks, G.R., 2016a. A varve record of Lake Ojibway glaciolacustrine deposits from Lac Dasserat, northwestern Quebec, Canada; Geological Survey of Canada, Open File 8089, 1 .zip file. doi:10.4095/299013
- Brooks, G.R., 2016b. Reconnaissance sub-bottom profiling survey at Lac Opastica, Quebec. Open File 7984, Geological Survey of Canada, Ottawa.  
doi:10.4095/297464
- Brooks, G.R. Medioli, B.E. 2012. Sub-bottom profiling and coring of sub-basins along the lower French River, Ontario; insights into depositional environments within the North Bay outlet. *Journal of Paleolimnology* 47, 447–467. DOI: 10.1007/s10933-010-9414-8.
- Chapron, E., Beck, C., Pourchet, M., Deconinck, J.-F., 1999. 1822 earthquake-triggered homogenite in Lake Le Bourget (NW Alps). *Terra Nova* 11, 86-92.
- Daubois, V., Roy, M., Veillette, J.J., Ménard, M., 2015. The drainage of Lake Ojibway in glaciolacustrine sediments of northern Ontario and Quebec, Canada. *Boreas* 44, 305-318.
- Dionne, J.C., 1977. Relict iceberg furrows on the floor of glacial Lake Ojibway, Québec and Ontario. *Atlantic Geology* 13, 79-81.
- Doig, R., 1990. 2300 yr history of seismicity from silting events in Lake Tadoussac, Charlevoix, Quebec. *Geology* 18, 820-823.
- Doig, R., 1998. 3000-year paleoseismological record from the region of the 1988 Saguenay, Quebec, earthquake. *Bulletin of the Seismological Society of America* 88, 1198-1203.
- Doughty, M., Eyles, N., Daurio, L., 2010. Earthquake-triggered slumps (1935 Timiskaming M6.2) in Lake Kipawa, Western Quebec Seismic Zone, Canada. *Sedimentary Geology* 228, 113–118, <http://dx.doi.org/10.1016/j.sedgeo.2010.04.003>.

- Doughty, M., Eyles, N., Eyles, C.H., 2013. High-resolution seismic reflection profiling of neotectonic faults in Lake Timiskaming, Timiskaming Graben, Ontario-Quebec, Canada. *Sedimentology* 60, 983-1006.
- Doughty, M., Eyles, N., Eyles, C.H., Wallace, K., Boyce, J.I., 2014. Lake sediments as natural seismographs: Earthquake-related deformations (seismites) in central Canadian lakes. *Sedimentary Geology* 313, 45-67.
- Dyke, A.S., Moore, A., Roberston, L., 2003. Deglaciation of North America. Open File 1574. Geological Survey of Canada, Ottawa.
- Eyles, N., Zajch, A., Doughty, M., 2015. High-resolution seismic sub-bottom reflection record of low hypsithermal lake levels in Ontario lakes. *Journal of Great Lakes Research* 41, 41-52.
- Girard I., Klassen R.A., Laframboise R.R., Lindsay P.J., 2004. Sedimentology laboratory manual, Terrain Sciences Division. Open File Report 4823. Geological Survey of Canada, Ottawa.
- Gouin, P., 2001. Tremblements de terre historiques au Québec: de 1534 à mars 1925, identifiés et interprétés à partir des textes originaux contemporains – Historical earthquakes felt in Quebec: from 1534 to March 1925, as revealed by the local contemporary literature. Guérin Éditeur Itée, Montreal.
- Hardy, L., 1982. Le Wisconsinien supérieur à l'est de la baie James (Québec). *Naturaliste Canadien* 109, 333-351.
- Hughes, O.L., 1959. Surficial geology of Smooth Rock and Iroquois Falls map areas, Cochrane District, Ontario: Department of Geology, University of Kansas, unpublished Ph.D. thesis.
- Hughes, O.L., 1965. Surficial geology of part of the Cochrane District, Ontario, Canada. In: Wright Jr., H.E., Frey, D.G. (Eds.), *International Studies on the Quaternary INQUA U.S.A. Geological Society of America, Special Paper 84*, pp. 535-565.
- Jibson, R.W., 2009. Using landslides for paleoseismic analysis. In: McCalpin, J.P. (Ed.), *Paleoseismology*, 2<sup>nd</sup> edition, *International Geophysics* 95, pp. 565-601.
- Johnston, A.C., 1996. A wave in the earth. *Science* 274, 735.
- Karlin, R.E., Holmes, M., Abella, S.E.B., Sylwester, R., 2004. Holocene landslides and a 3500-year record of Pacific Northwest earthquakes from sediments in Lake Washington. *Geological Society of America Bulletin* 116, p. 94–108, <http://dx.doi.org/10.1130/B25158.1>.
- Kaszycki, C.A., 1987. A model for glacial and proglacial sedimentation in the shield terrane of southern Ontario. *Canadian Journal of Earth Sciences* 24, 2373-2391.
- Klassen, R.A., Shilts, W.W., 1982. Subbottom profiling of lakes of the Canadian Shield. *Current Research, Part A, Paper 82-1A*. Geological Survey of Canada, Ottawa, pp. 375-384.

- Kremer, K., Hilbe, M., Simpson, G., Decrouy, L., Wildi, W., Girardclos, S., 2015. Reconstructing 4000 years of mass movement and tsunami history in a deep peri-Alpine lake (Lake Geneva, France-Switzerland). *Sedimentology* 62, 1305-1327.
- Lagerbäck, R., 1990. Late Quaternary faulting and paleoseismicity in northern Fennoscandia, with particular reference to the Lansjärv area, northern Sweden. *Geologiska Föreningens / Stockholm Förhandlingar* 112, 333-354.
- Lajeunesse, P., Sinkunas, B., Morissette, A., Normandeau, A., Joyal, G., St-Onge, G., Locat, J., 2016. Large-scale seismically-induced mass-movements in a former glacial lake basin: Lake Témiscouata, northeastern Appalachians (eastern Canada). *Marine Geology*. <http://dx.doi.org/10.1016/j.margeo.2016.04.007>.
- Lamontagne, M., Halchuk, S., Cassidy, J.F., Rogers, G.C., 2008. Significant Canadian earthquakes of the period 1600–2006. *Seismological Research Letters* 79, 211-223.
- Lamoureux, S., 2001. Varve chronology techniques, In: Last, W.M., Smol, J.P., (Eds.), *Tracking environmental change using lake sediments. Volume 1. Basin analysis, coring, and chronological techniques*. Kluwer Academic Publishers, Dordrecht, pp. 247-259.
- Lazorek, M., Eyles, N., Eyles, C.H., Doughty, M., L'Heureux, E., Milkereit, B. 2006. Late Quaternary seismo-stratigraphy of Lake Wanapitei, Sudbury, Ontario, Canada: arguments for a possible meteorite impact origin. *Sedimentary Geology* 192, 231-242.
- Livingstone, D.A. 1955. A lightweight piston sampler for lake deposits. *Ecology* 36, 137-139.
- Lundqvist, J., Lagerbäck, R., 1976. The Parve Fault; a late-glacial fault in the Precambrian of Swedish Lapland. *Geologiska Föreningens / Stockholm Förhandlingar* 98, 45-51.
- Michetti, A.M. et al., 2015. Environmental Seismic Intensity scale - ESI 2007. *Memorie descrittive della carta geologica d'Italia* 97, 11-20.
- Moernaut, J., De Batist, M., Charlet, F., Heirman, K., Chapron, E., Pino, M., Brümmer, R., Urrutia, R., 2007. Giant earthquakes in South-Central Chile revealed by Holocene mass-wasting events in Lake Puyehue. *Sedimentary Geology* 195, 239–256. <http://dx.doi.org/10.1016/j.sedgeo.2006.08.005>.
- Moernaut, J., Daele, M.V., Heirman, K., Fontijn, K., Strasser, M., Pino, M., Urrutia, R., De Batist, M., 2014. Lacustrine turbidites as a tool for quantitative earthquake reconstruction: New evidence for a variable rupture mode in south central Chile. *Journal of Geophysical Research: Solid Earth* 119, 1607-1633.
- Monecke, K., Anselmetti, F.S., Becker, A., Schnellmann, M., Sturm, M., Giardini, D., 2006. Earthquake-induced deformation structures in lake deposits: A Late Pleistocene to Holocene paleoseismic record for Central Switzerland. *Eclogae Geologicae Helvetiae* 99, 343–362. <http://dx.doi.org/10.1007/s00015-006-1193-x>.

- Morey, A.E., Goldfinger, C., Briles, C.E., Gavin, D.G., Colombaroli, D., Kusler, J.E., 2013. Are great Cascadia earthquakes recorded in the sedimentary records from small forearc lakes? *Natural Hazards and Earth Systems Science* 13, 2441–2463.  
<http://dx.doi.org/10.5194/nhess-13-2441-2013>.
- Mörner, N.-A., 2003. Paleoseismicity of Sweden: a novel paradigm: a contribution to INQUA from its sub-commission on paleoseismicity. Stockholm University, Stockholm.
- Mörner, N.-A., 2004. Active faults and paleoseismicity in Fennoscandia, especially Sweden: primary structures and secondary effects. *Tectonophysics* 380, 139-157.
- Mörner, N.-A., 2005. An interpretation and catalogue of paleoseismicity in Sweden. *Tectonophysics* 408, 265-307.
- Nomade, J., Chapron, E., Desmet, M., Reyss, J.-L., Arnaud, F., Lignier, V., 2005. Reconstructing historical seismicity from lake sediments (Lake Laffrey, Western Alps, France). *Terra Nova* 17, 350-357.
- Normandeau, A., Lajeunesse, P., Philibert, G., 2013. Late-Quaternary morphostratigraphy of Lake St-Joseph (southeastern Canadian Shield): Evolution from a semi-enclosed glacial marine basin to a postglacial lake. *Sedimentary Geology* 295, 38-52.
- Ouellet, M., 1997. Lake sediments and Holocene seismic hazard assessment within the St. Lawrence Valley, Quebec. *Geological Society of America Bulletin* 109, 631-642.
- Owen, G., Moretti, M., Alfaro, P., 2011. Recognising triggers for soft-sediment deformation: Current understanding and future directions. *Sedimentary Geology* 235, 133-140.
- Praet, N., Moernaut, J., Van Daele, M., Boes, E., Haeussler, P.J., Strupler, M., Schmidt, S., Loso, M.G., De Batist, M., 2016. Paleoseismic potential of sublacustrine landslide records in a high-seismicity setting (south-central Alaska). *Marine Geology*.  
<http://dx.doi.org/10.1016/j.margeo.2016.05.004>
- Rayburn, J.A., Vollmer, F.W., 2013. ANTEVS: A quantitative varve sequence cross-correlation technique with examples from the northeastern United States. *GFF: Journal of the Geological Society of Sweden* 135, 282-292.
- Roy, M., Dell'Oste, F., Veillette, J.J., de Vernal, A., Hélie, J.F., Parent, M., 2011. Insights on the events surrounding the final drainage of Lake Ojibway based on James Bay stratigraphic sequences. *Quaternary Science Reviews* 30, 682-692.
- Roy, M., Veillette, J.J., Daubois, V., Ménard, M., 2015. Late-stage phases of glacial Lake Ojibway in the central Abitibi region, eastern Canada. *Geomorphology* 248, 14-23.
- Schnellmann, M., Anselmetti, F.S., Giardini, D., McKenzie, J.A., Ward, S.N., 2002. Prehistoric earthquake history revealed by lacustrine slump deposits. *Geology* 30, 1131–1134.  
[http://dx.doi.org/10.1130/0091-7613\(2002\)030](http://dx.doi.org/10.1130/0091-7613(2002)030).

- Schnellmann, M., Anselmetti, F.S., Giardini, D., McKenzie, J.A., 2006. 15,000 Years of mass-movement history in Lake Lucerne: implications for seismic and tsunami hazards. *Eclogae Geologicae Helvetiae* 99, 409–428. <http://dx.doi.org/10.1007/s00015-006-1196-7>.
- Shilts, W.W., 1984. Sonar evidence of postglacial tectonic instability of the Canadian Shield and Appalachians. In: *Current Research, Part A, Paper 84-1A*. Geological Survey of Canada, Ottawa, pp. 567-579.
- Shilts, W.W., Clague, J.J., 1992. Documentation of earthquake-induced disturbance of lake sediments using subbottom acoustic profiling. *Canadian Journal of Earth Sciences* 29, 1018-1042.
- Shilts, W.W., Rappol, M., Blais, A., 1992. Evidence of late and postglacial seismic activity in the Témiscouata -Madawaska Valley, Quebec-New Brunswick, Canada. *Canadian Journal of Earth Sciences* 29, 1043-1069.
- Siegenthaler, C., Finger, W., Kelts, K., Wang, S., 1987. Earthquake and seiche deposits in Lake Lucerne, Switzerland. *Eclogae Geologicae Helvetiae* 80, 241-260.
- Sims, J.D., 2012. Earthquake-induced load casts, pseudonodules, ball-and-pillow structures, and convolute lamination; additional deformation structures for paleoseismic studies. In: Cox, R.T., Tuttle, M.P., Boyd, O.S., Locat, J. (Eds.), *Recent advances in North American paleoseismology and neotectonics east of the Rockies*. Geological Society of America, Special Paper 493: 191-201.
- Smith, C.A., Sundh, M., Mikko, H., 2014. Surficial geology indicates early Holocene faulting and seismicity, central Sweden. *International Journal of Earth Sciences* 103, 1711-1724.
- Smith, S.B., Karlin, R.E., Kent, G.M., Seitz, G.G., Driscoll, N.W., 2013. Holocene subaqueous paleoseismology of Lake Tahoe. *Geological Society of America Bulletin* 125, 691-708.
- Stewart, I.S., Sauber, J. Rose, J., 2000. Glacio-seismotectonics: ice sheets, crustal deformation and seismicity. *Quaternary Science Reviews* 19, 1367-1389.
- Strasser, M., Anselmetti, F.S., Fäh, D., Giardini, D., Schnellmann, M., 2006. Magnitudes and source areas of large prehistoric northern alpine earthquakes revealed by slope failures in lakes. *Geology* 34, 1005–1008. <http://dx.doi.org/10.1130/G22784A.1>.
- Strasser, M., Monecke, K., Schnellmann, M., Anselmetti, F.S., 2013. Lake sediments as natural seismographs: A compiled record of Late Quaternary earthquakes in Central Switzerland and its implication for Alpine deformation. *Sedimentology* 60, 319–341. <http://dx.doi.org/10.1111/sed.12003>.
- Stroup, J.S., Lowell, T.V., Breckenridge, A., 2013. A model for the demise of large, glacial Lake Ojibway, Ontario and Quebec. *Journal of Paleolimnology* 50, 105-121.
- Upton, P., Osterberg, E.C., 2007. Paleoseismicity and mass movements interpreted from seismic-reflection data, Lake Tekapo, South Canterbury, New Zealand. *Journal of Geology and Geophysics* 50, 343–356. <http://dx.doi.org/10.1080/00288300709509841>.

- Veillette, J.J., 1983. Déglaciation de la vallée supérieure de l'Outaouais, le lac Barlow et le sud du lac Ojibway, Québec. *Géographie physique et Quaternaire* 37, 67-84.
- Veillette, J.J., 1994. Evolution and paleohydrology of glacial Lakes Barlow and Ojibway. *Quaternary Science Reviews* 13, 945-971.
- Veillette, J.J., Paradis, S.J., 1996. Iceberg furrows as paleowind indicators and icebergs as erosion and sedimentation agents in Glacial Lake Ojibway, Abitibi, Québec. Open File 3031. Geological Survey of Canada, Ottawa. doi: 10.4095/205754.
- Veillette, J.J., Paradis, S.J., Thibaudeau, P., 2010. Surficial geology, Rouyn-Noranda–Senneterre, Quebec/Géologie des formations superficielles, Rouyn-Noranda–Senneterre, Québec. Open File 6061. Geological Survey of Canada, Ottawa.
- Vincent, J.-S., Hardy, L., 1979. The evolution of glacial lakes Barlow and Ojibway, Quebec and Ontario. Bulletin 316. Geological Survey of Canada, Ottawa.
- Vollmer, F.W., 2014. ANTEVS: Automatic numerical time-series evaluation of varying sequences software. Retrieved on June 23, 2015 from: [www.frederickvollmer.com/antevs](http://www.frederickvollmer.com/antevs).
- Zolitschka, B., Francus, P., Ojala, A.E.K., Schimmelmann, A., 2015. Varves in lake sediments – a review. *Quaternary Science Reviews* 117, 1-41.